AD_____

Award Number: W81XWH-08-1-0453

TITLE: Development of Mouse Models of Ovarian Cancer for Studying Tumor Biology and Testing Novel Molecularly Targeted Therapeutic Strategies.

PRINCIPAL INVESTIGATOR: Kathleen R. Cho, M.D.

CONTRACTING ORGANIZATION: University of Michigan
Ann Arbor, MI 48109-1274

REPORT DATE: September 2011

TYPE OF REPORT: Final

PREPARED FOR: U.S. Army Medical Research and Materiel Command
Fort Detrick, Maryland 21702-5012

REPORT DOCUMENTATION PAGE

Form Approved
OMB No. 0704-0188

1. REPORT DATE	2. REPORT TYPE	3. DATES COVERED
September 2011	Final	1 July 2008 – 30 June 2011

4. TITLE AND SUBTITLE

Development of Mouse Models of Ovarian Cancer for Studying Tumor Biology and Testing Novel Molecularly Targeted Therapeutic Strategies.

5a. CONTRACT NUMBER

5b. GRANT NUMBER
W81XWH-08-1-0453

5c. PROGRAM ELEMENT NUMBER

6. AUTHOR(S)

Kathleen R. Cho
Alnawaz Rehemtulla

E-Mail: kathcho@umich.edu

5d. PROJECT NUMBER

5e. TASK NUMBER

5f. WORK UNIT NUMBER

7. PERFORMING ORGANIZATION NAME(S) AND ADDRESS(ES)

University of Michigan
Ann Arbor, MI 48109-1274

8. PERFORMING ORGANIZATION REPORT NUMBER

9. SPONSORING / MONITORING AGENCY NAME(S) AND ADDRESS(ES)
U.S. Army Medical Research and Materiel Command
Fort Detrick, Maryland 21702-5012

10. SPONSOR/MONITOR'S ACRONYM(S)

11. SPONSOR/MONITOR'S REPORT NUMBER(S)

12. DISTRIBUTION / AVAILABILITY STATEMENT
Approved for Public Release; Distribution Unlimited

13. SUPPLEMENTARY NOTES

14. ABSTRACT
The objective of this project was to create genetically engineered mouse (GEM) models that in addition to developing ovarian carcinomas similar to human endometrioid carcinomas, also express a reporter for Caspase-3 activity, a hallmark of cells undergoing apoptosis. During the three year funding period, we generated stable lines of transgenic mice carrying a Cre-inducible luciferase reporter ($ROSA26^{LSL\text{-}Luc}$) or apoptosis reporter ($Apoptosis^{LSL\text{-}Luc}$) and verified function of the reporter transgenes in vivo. Using $Apc^{flox/flox}$;$Pten^{flox/flox}$;$ROSA26^{LSL\text{-}Luc/+}$ and Apcflox/flox;Ptenflox/flox;ApoptosisLSL-Luc mice generated as part of this project, we demonstrated that bioluminescence imaging can be used to monitor ovarian tumor progression and drug response in vivo. In addition, we showed that $Apc^{flox/flox}$;$Pten^{flox/flox}$;$Apoptosis^{LSL\text{-}Luc}$ mice can be used to image treatment-dependent induction of apoptosis. Efficacy of a targeted therapeutic agent (Akt inhibitor, Perifosine), alone and in combination with a standard chemotherapeutic agent (Cisplatin) was evaluated. Our studies revealed that combination therapy resulted in enhanced levels of apoptosis compared to either agent alone, and suggest this may be a promising approach for treating women with advanced stage ovarian endometrioid adenocarcinomas with PI3K/Akt/mTOR signaling pathway defects.

15. SUBJECT TERMS
ovarian endometrioid adenocarcinoma, transgenic mouse model, functional imaging reporter

16. SECURITY CLASSIFICATION OF:			17. LIMITATION OF ABSTRACT	18. NUMBER OF PAGES	19a. NAME OF RESPONSIBLE PERSON
a. REPORT	b. ABSTRACT	c. THIS PAGE			USAMRMC
U	U	U	UU	33	19b. TELEPHONE NUMBER *(include area code)*

Table of Contents

INTRODUCTION:

A goal of ovarian cancer research is to identify "hallmark" genetic alterations that characterize each major histological subtype of ovarian carcinoma and to develop novel therapeutics that target the signaling pathways deregulated by these molecular defects. Ideally, "personalized" therapeutic regimens could be designed based on the specific molecular alterations present in a given patient's tumor. Molecular data collected over the last several years have led to better comprehension of cancer pathogenesis and the mechanisms by which deregulated signaling pathways contribute to tumor development and progression. These pathways offer novel therapeutic 'targets' (e.g. Akt) for 'lead molecules' designed to inhibit the signaling derived from these pathways. Our ability to efficiently translate new therapies from the laboratory bench into the patient would be greatly enhanced by the availability of animal models that could be used to test efficacy of new drugs, evaluate their toxicity, and identify the best route of administration, dose, and schedule. Only limited information can be obtained from the response of cancer cells in culture or implanted (xenografted) into immuno-compromised mice. Although there are many new drugs and possible combinations of drugs available today, identification of the most efficacious of these remains a major challenge and a rate- limiting process that cannot easily be conducted in women with the disease. Molecular imaging technologies have the potential to enhance preclinical studies conducted in animal models of cancer. As imaging methods are non-invasive, they allow for longitudinal studies in a single animal. Moreover, molecular imaging can increase the statistical significance of a study, allow for more clinically relevant study designs and decrease the number of animals required. Imaging in live animals can also provide important information on the optimal route of delivery, timing, and dosing of drugs. Dr. Cho's group has developed a mouse model of ovarian endometrioid adenocarcinoma, based on conditional deletion of *Apc* and *Pten*, which shows morphological features, biological behavior, and gene expression profiles similar to human endometrioid adenocarcinomas with the same signaling pathway defects[1]. In parallel, Dr. Rehemtulla's group has developed several molecular imaging strategies for non-invasive monitoring of Akt kinase activity as well as Caspase-3 proteolytic activity in live animals[2,3]. The objective of this project is to combine these two technologies to create genetically engineered mouse (GEM) models that in addition to developing ovarian carcinomas, will also express either a reporter for Akt activity, a major survival signal, or for Caspase-3 activity, a hallmark of cells undergoing apoptosis. We hypothesize that tumors arising in our GEM model of ovarian cancer will respond to drugs that target the specific molecular defects present in the tumor cells, and that response to different drug regimens can be monitored quantitatively and non-invasively in live animals.

BODY:

As described below, we have completed nearly all of the tasks outlined in the Statement of Work (SOW) proposed in our original application. The laboratories of the Initiating PI (Cho) and Partnering (Rehemtulla) PI have worked very closely together to complete the majority of the tasks outlined in the SOW, and hence, progress from both labs during the three year funding period will be summarized below with specific contributions of each lab toward individual tasks clearly indicated. Our studies have emphasized work with the $Rosa26^{LSL\text{-}Luc}$ and $Apoptosis^{LSL\text{-}Luc}$ reporters, as $Apc^{flox/flox}$;$Pten^{flox/flox}$ mice carrying these reporter transgenes were successfully generated relatively early in the funding period.

Summary of research accomplishments associated with each task outlined in the approved Statement of Work:

Aim 1

Task 1: Finish construction of reporter cassettes, sequence verify (**completed**, **year 1 –** Rehemtulla laboratory)

Task 2: Functional validation of constructs in vitro (**completed, year 1** - Rehemtulla laboratory)

Task 3: Plasmid DNA purification for injection, microinjection of mouse eggs and surgical transfer to recipients, screen potential founders (**completed, year 1** - UM transgenic animal core facility and Rehemtulla laboratory)

Task 4: Cross founder mice to C57BL/6 mice to verify germline transmission of reporter transgenes, breed to homozygosity (**completed, year 1** for Apoptosis$^{LSL\text{-}Luc}$ and *Rosa26*$^{LSL\text{-}Luc}$ reporters, Rehemtulla and Cho laboratories)

Task 5: Determine transgene copy number, verify expression of *tomato* by bioluminescence imaging (BLI), verify Cre recombination-dependent loss of *tomato* and activation of *renilla*luc and *firefly*luc activity in vivo (**completed, year 2** for Apoptosis reporter, Rehemtulla laboratory)

Task 6: Cross each reporter mouse line to *Apc*$^{flox/flox}$*;Pten*$^{flox/flox}$ mice to generate triple transgenic animals (**completed, year 2** for Apoptosis$^{LSL\text{-}Luc}$ reporter, Cho and Rehemtulla laboratories and *Rosa26*$^{LSL\text{-}Luc}$ reporter, Cho laboratory)

Task 7: Validation of triple transgenic lines for tumor formation and reporter expression after ovarian bursal AdCre injection (**completed, year 2** for *Rosa26*$^{LSL\text{-}Luc}$ reporter, Cho laboratory and **completed, year 3** for Apoptosis$^{LSL\text{-}Luc}$ reporter, Cho and Rehemtulla laboratories)

Aim2

Task 8: Ovarian bursal injection of AdCre for generation of tumor bearing mice expressing functional imaging reporters (**completed years 2 and 3,** Cho laboratory)

Task 9: Treatment of tumor-bearing mice with cisplatin accompanied by MRI and BLI (**completed years 2 and 3,** Rehemtulla and Cho laboratories)

Task 10: Treatment of tumor-bearing mice with perifosine accompanied by MRI and BLI (**completed, years 2 and 3**, Rehemtulla and Cho laboratories).

Task 11: Treatment of tumor-bearing mice with SC-560 accompanied by MRI and BLI (**not performed**)

Task 12: Histological and immunohistochemical analysis of β-catenin, Pten, pAkt, pS6, etc., in control and treated tumors (**completed, year 3,** Cho laboratory)

Task 13: Biochemical (immunoblot) analysis of β-catenin, Pten, pAkt, pS6, etc., in control and treated tumors (**completed, year 3,** Cho laboratory).

Aim 3

Task 14: Treatment of tumor-bearing animals with combination therapy (**completed years 2 and 3,** Rehemtulla and Cho laboratories

Task 15: Histological and immunohistochemical analysis of β-catenin, Pten, pAkt, pS6, etc., in control and combination-treated tumors (**in progress,** Rehemtulla and Cho laboratories)

Task 16: Biochemical (immunoblot) analysis of β-catenin, Pten, pAkt, pS6, etc., in control and combination-treated tumors (**in progress,** Rehemtulla and Cho laboratories).

Task 17: Treatment of tumor-bearing animals with optimal combination therapy with varying schedules, accompanied by MRI and BLI (**in progress,** Rehemtulla and Cho laboratories)

A detailed description of studies performed toward completion of the specific tasks in the SOW is provided below:

Aim 1: Construction of transgenic mice wherein conditional deletion of *Apc* and *Pten* occurs with simultaneous expression of molecular imaging reporters for Akt or Apoptosis.

(i) Construction of reporter transgenic mice: As described in our Annual Reports for years 1 and 2, we proposed to construct two transgenic mice strains wherein expression of a molecular imaging reporter (Apoptosis or Akt) as well as an internal control can be activated in a *Cre* dependent manner. The Rehemtulla laboratory designed the transgene constructs to contain the EF-1 (PEF) promoter which drives transcription of the *tomato* (fluorescent protein) coding sequence. The presence of a transcription stop site and poly-adenylation target site (pA) at the end of the *tomato* coding sequence result in termination of transcription such that only the tomato protein is expressed. In the presence of *Cre* recombinase (ectopically expressed), recombination of the *loxP* sequences would result in deletion of the *tomato* coding sequence as well as the adjoining pA sequences. In this "floxed" form, the transgene results in transcription of the molecular imaging (Akt or apoptosis) firefly luciferase reporter as well as an IRES (internal ribosome entry site) and the *renilla* luciferase (*r*luc) coding sequence **(Figure 1).**

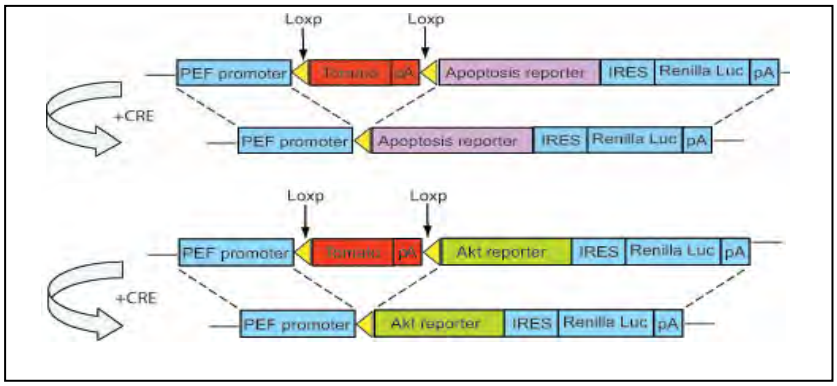

Figure 1. Diagram showing design of the constructs that allow for conditional activation of the Akt (Akt$^{LSL\text{-}Luc}$**) and Apoptosis (**Apoptosis$^{LSL\text{-}Luc}$**) reporters**.

In our previous Annual Reports, we described the generation of *Apoptosis*$^{LSL\text{-}Luc}$ reporter mice and presented data showing that the Apoptosis$^{LSL\text{-}Luc}$ reporter transgene can be conditionally activated under conditions in which Cre is expressed in a tissue-specific manner. Having validated proper function of the *Apoptosis*$^{LSL\text{-}Luc}$ reporter in vitro and in vivo, and given the relatively short (3 year) time frame of this project, we opted to pursue our remaining work using *Apc*$^{flox/flox}$*;Pten*$^{flox/flox}$ mice expressing either the *Rosa26*$^{LSL\text{-}Luc}$ or *Apoptosis*$^{LSL\text{-}Luc}$ reporter transgenes, and discontinued further development of mice expressing a functional Akt reporter.

(ii) *Mating of the transgenic reporter mice with Apc*$^{flox/flox}$*;Pten*$^{flox/flox}$ *mice:*

During years 2 and 3, we successfully generated sufficient numbers of *Apc*$^{flox/flox}$*;Pten*$^{flox/flox}$*;* *Apoptosis*$^{LSL\text{-}Luc}$ and *Apc*$^{flox/flox}$*;Pten*$^{flox/flox}$*;Rosa26*$^{LSL\text{-}Luc/+}$ mice for use in work proposed in Aims 2 and 3.

(iii) Characterization of the transgenic reporter mice developed above:

Our year 2 Annual Report described studies confirming that BLI can be used to monitor ovarian tumor progression over time in *Apc*$^{flox/flox}$*;Pten*$^{flox/flox}$*;Rosa26*$^{LSL\text{-}Luc/+}$ mice. Similar work has been performed in *Apc*$^{flox/flox}$*;Pten*$^{flox/flox}$*; Apoptosis*$^{LSL\text{-}Luc}$ mice during the final year of the funding period (see below).

Aim 2: Molecular imaging of single-agent therapeutic efficacy in a mouse ovarian endometrioid adenocarcinoma (OEA) model.

We have essentially completed the tasks associated with this Aim. A paper describing our findings has recently been published in *Clinical Cancer Research* (see attached reprint, R. Wu et al., *Clinical Cancer Research*, 17(23):7359-72, 2011, Appendix 1). Publication of this paper led to an invitation to contribute a "Feature" piece in the journal *Cell Cycle* (see attached email from *Cell Cycle* editor, Mikhail Balgosklonny, Appendix 3 [new]).

Briefly, OEAs were induced by injection of adenovirus expressing Cre recombinase (AdCre) into the ovarian bursae of $Apc^{flox/flox}$;$Pten^{flox/flox}$; $Rosa26^{LSL\text{-}Luc/+}$ mice. Tumor-bearing mice or murine OEA-derived cell lines were treated with cisplatin and paclitaxel, mTOR inhibitor rapamycin, or AKT inhibitors API-2 or perifosine. Treatment effects were monitored in vivo by tumor volume measurements and bioluminescence imaging, in vitro by WST-1 proliferation assays, and in OEA tissues and cells by immunoblotting and immunostaining for levels and phosphorylation status of PI3K/AKT/mTOR signaling pathway components. We found that murine OEAs responded to cisplatin and paclitaxel, rapamycin, and AKT inhibitors in vivo (appended publication, Figure 5). In vitro studies showed that response to mTOR and AKT inhibitors, but not conventional cytotoxic drugs, was dependent on the status of PI3K/AKT/mTOR signaling (appended publication, Figure 3). We also found that PI3K/AKT/mTOR pathway inhibition in APC-/PTEN- tumor cells resulted in compensatory up-regulation of ERK signaling (appended publication, Supplemental Figure S2A), suggesting that multiple rather than single agent targeted therapy will be more efficacious for treating ovarian cancers. The studies clearly demonstrate the utility of this GEM model of ovarian cancer for preclinical testing of novel PI3K/AKT/mTOR signaling inhibitors. Methodological details and data figures are provided in the attached reprint.

In further response to the Reviewer's request for more comprehensive description of work accomplished for Aim 2, specific data elements (page number, and/or figure number) in the appended publication (R Wu et al., *Clinical Cancer Research*, 17(23):7359-72, 2011) that support our research findings are detailed below. The appended publication (Appendix 1) now also includes supplemental data and figure legends.

Aim2

Task 8: Ovarian bursal injection of AdCre for generation of tumor bearing mice expressing functional imaging reporters (**completed years 2 and 3,** Cho laboratory): Methods describing tumor induction by AdCre injection are specified in appended publication, p. 7360.

Task 9: Treatment of tumor-bearing mice with cisplatin accompanied by MRI and BLI (**completed years 2 and 3,** Rehemtulla and Cho laboratories). Methods describing treatment of mice with cisplatin are specified in appended publication, p. 7361; data showing response of tumor-bearing mice to cisplatin and paclitaxel are provided in Figure 5D. Methods for BLI are specified on p. 7362; data showing representative BLI data are provided in Figure 5E. Representative MRI data are shown in description of Aim 3.

Task 10: Treatment of tumor-bearing mice with perifosine accompanied by MRI and BLI (**completed, years 2 and 3**, Rehemtulla and Cho laboratories). Methods describing treatment of mice with perifosine are specified in appended publication, p. 7361; data showing response of tumor-bearing mice to perifosine are provided in Figure 5C. Methods for BLI are specified on p. 7362; data showing representative BLI data are provided in Figure 5E. Representative MRI data are shown in description of Aim 3.

Task 11: Treatment of tumor-bearing mice with SC-560 accompanied by MRI and BLI (**not performed**)

Task 12: Histological and immunohistochemical analysis of β-catenin, Pten, pAkt, pS6, etc., in control and treated tumors (**completed, year 3,** Cho laboratory). Methods describing immunohistochemical analysis of murine ovarian tumors are specified in appended publication, p. 7361. Representative data showing immunohistochemical analysis of treated and untreated tumors are shown in Supplemental Figure S3.

Task 13: Biochemical (immunoblot) analysis of β-catenin, Pten, pAkt, pS6, etc., in control and treated tumors (**completed, year 3,** Cho laboratory). Methods describing immunoblot analysis of drug treated murine tumor cell lines are specified in appended publication, p. 7361. Representative data showing representative immunoblot analysis of drug-treated murine tumor cells are shown in Figure 4 and Supplemental Figure S2.

Aim 3: Optimization of combination therapies using molecular imaging.

Anti-cancer drug discovery efforts are aimed at selecting, from a vast number of candidate compounds, those that most safely and effectively eradicate the disease. Moreover, given the overwhelming number of possible combination therapies that can be considered for evaluation in clinical trials, animal model systems can be used to identify those multi-drug regimens with greatest promise for efficacy in humans. In Specific Aim 3 we had proposed to use molecular imaging to identify the most efficacious combination therapy. Since platinum-based agents (Carbo- and Cisplatin) are the standard of care for ovarian cancer, we wanted to investigate if inhibition of the key survival signaling pathway (i.e. the PI-3-Kinase/Akt pathway) would enhance the efficacy of these platinum-based chemotherapies. Indeed, results presented in the figures below demonstrate that the ability to image apoptosis provides proof that the combination therapy has enhanced efficacy compared to single agents alone.

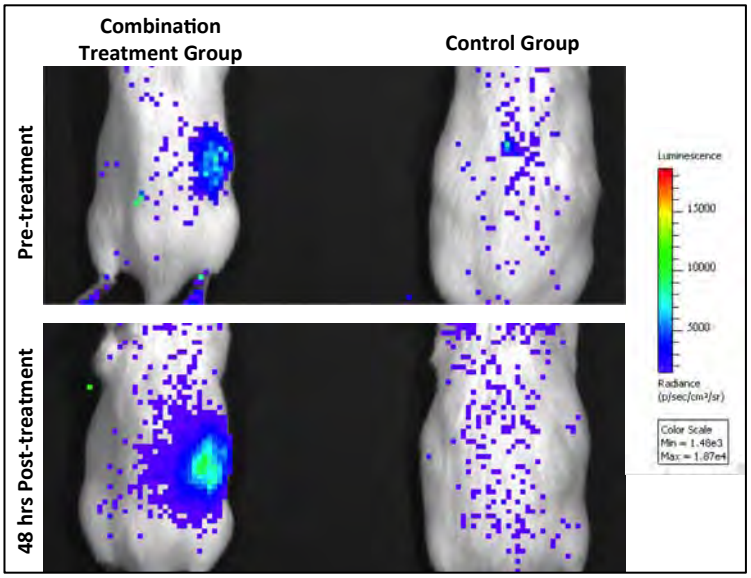

Figure 2: Imaging of Apoptosis in OEA tumor-bearing mice in response to combination therapy. Tumor-bearing mice that were also expressing the Apoptosis reporter were treated with Cisplatin 5mg/kg/, and Perifosine (10mg/kg/). In contrast to the Control group (untreated, right) the combination therapy (left) resulted in greatly increased apoptosis. Although only a single time point is shown here, when combined with data shown in Figure 3, our findings suggest that the combination therapy results in more than additive increase on apoptosis, and will be more efficacious.

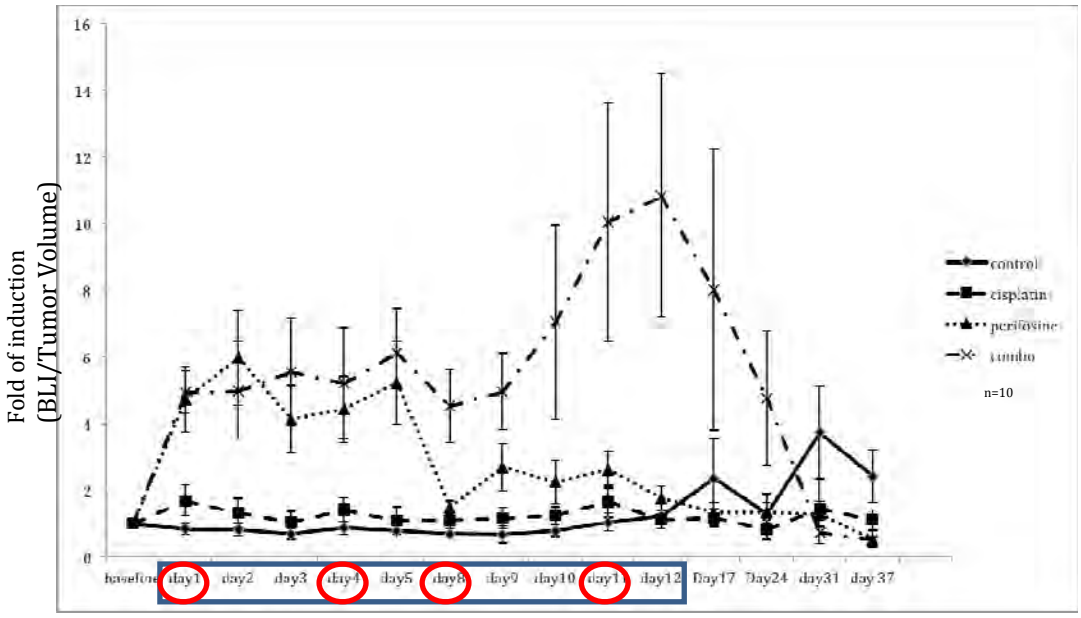

Figure 3: Molecular Imaging of Apoptosis Reveals Enhanced Efficacy when Cisplatin and Perifosine are combined compared to either drug as single agent. Tumor-bearing animals that also express the *Apoptosis*$^{LSL\text{-}Luc}$ reporter were used to evaluate the efficacy of combining an Akt-inhibitor (Perifosine) with Cisplatin. Control group was treated with PBS. The Perifosine group was treated with 10mg/kg Perifosine, 5 times a week for two weeks; The Cisplatin group was treated with 5mg/kg cisplatin given twice a week; combination group was treated with 5mg/kg cisplatin twice a week (circles) and 10mg/kg perifosine, 5 times a week for two weeks (box). Animals were monitored for 3 weeks after completion of therapy. Bioluminescence signals were monitored 5 times a week 6 hours after treatment. Averages of fold of increase in bioluminescence signals are plotted upon normalization to tumor volume change and error bars represent SEM.

These results demonstrate that Cisplatin treatment alone resulted in some induction of apoptosis, while Perifosine treatment alone resulted in a significantly more enhanced levels of apoptosis on the first five days of treatment which subsided for the following five days (days 8-12). We believe this may represent the development of resistance to the drug. Interestingly, when the animals were treated with Cisplatin and Perifosine in combination, the tumors continued to undergo apoptosis on days 8-12 and in fact, the level of apoptosis was significantly more robust. These results support our hypothesis that the combination therapy would be more efficacious than either agent alone.

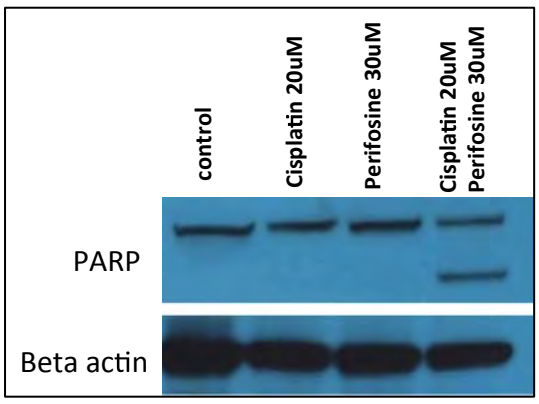

Figure 4: Biochemical validation of enhanced apoptosis in response to combination therapy. To demonstrate that results from the bioluminescence reporter are supported by an independent technique, we performed immunochemical assays. As shown by the western blot, combination therapy resulted in a robust activation of apoptosis as demonstrated by efficient cleavage of PARP (a known Caspase-3 substrate) which was not observed in response to cisplatin or perifosine alone.

In an effort to get an accurate alternative measure of tumor burden, we have utilized magnetic resonance imaging (MRI) of the *Apc*$^{flox/flox}$;*Pten*$^{flox/flox}$;*Apoptosis*$^{LSL\text{-}Luc}$ tumor-bearing mice (Figure 5).

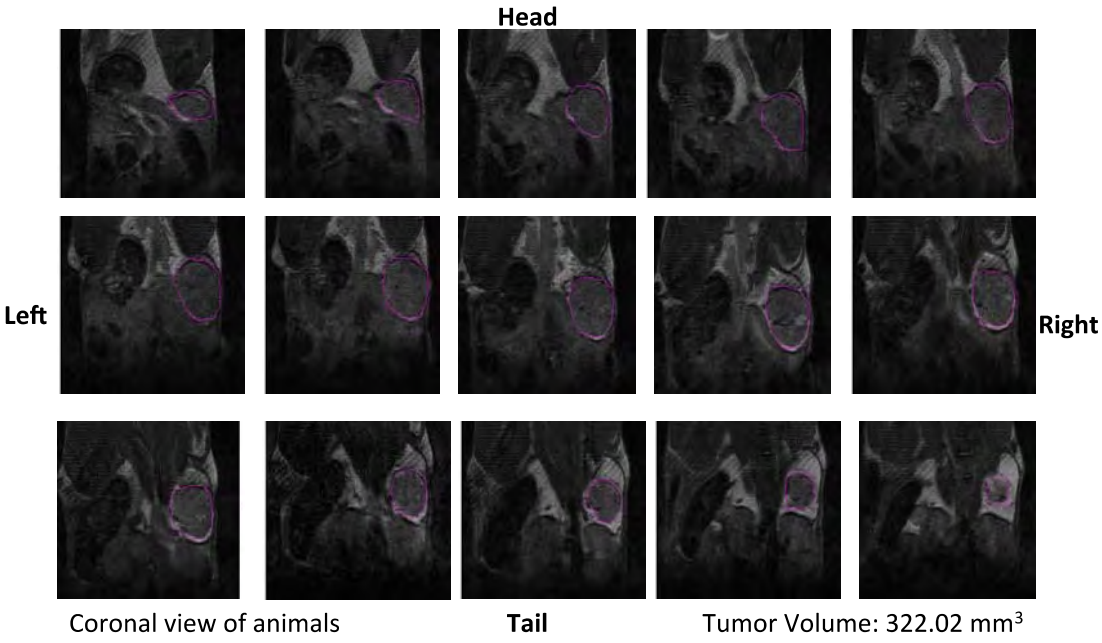

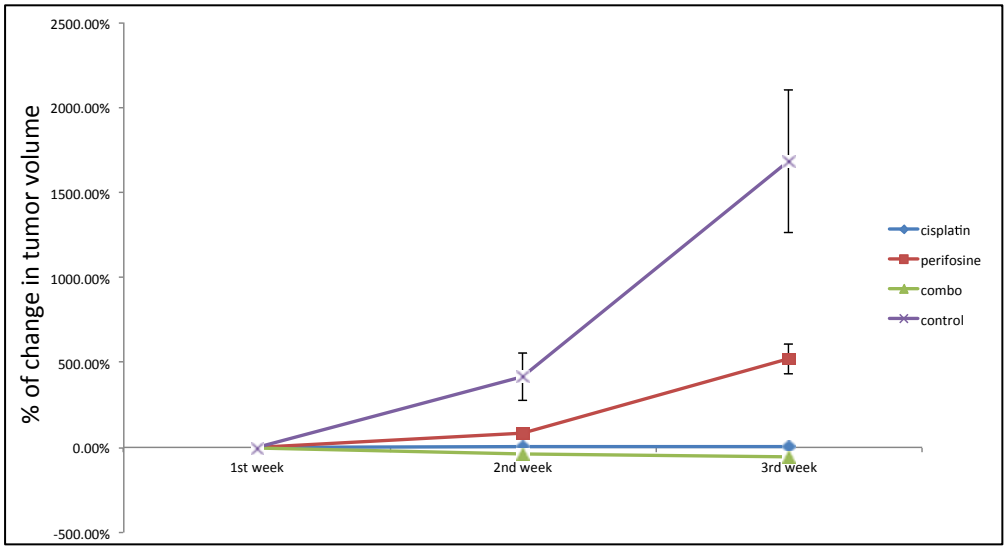

Figure 5: MRI can be used to monitor tumor burden and drug response in *Apc*$^{flox/flox}$;*Pten*$^{flox/flox}$;*Apoptosis*$^{LSL\text{-}Luc}$ mice. Upper panel: Sequential collection of coronal slices followed by circling of the OEA lesion (region of interest shown by red outline) reveals that this particular mouse had a 322 mm^3 tumor in the right ovary. Lower panel: change in tumor volume over time in tumor-bearing mice treated with vehicle, cisplatin, perifosine, or both, as measured by MRI.

KEY RESEARCH ACCOMPLISHMENTS:

- Generation of novel *Apoptosis*$^{LSL\text{-}Luc}$ transgenic reporter mouse strain.
- Generation of *Apc*$^{flox/flox}$*;Pten*$^{flox/flox}$*;Rosa26*$^{LSL\text{-}Luc/+}$ and *Apc*$^{flox/flox}$*;Pten*$^{flox/flox}$*;Apoptosis*$^{LSL\text{-}Luc}$ transgenic mice.
- Completion of proof-of-principle studies showing that bioluminescence imaging and MRI can be used to monitor ovarian tumor growth and response to molecularly targeted agents longitudinally over time in living animals.
- Proof-of-principle studies showing that these animals can be used to optimize combination therapies for ovarian cancer patients nearing completion.

REPORTABLE OUTCOMES:

Plenary presentation by Kathleen Cho (Initiating PI), "Mouse Models for Imaging Ovarian Cancer Progression and Therapeutic Response: Progress and Pitfalls", Japanese Society for Advancement of Women's Imaging (JSAWI), Annual Meeting, September, 2011, Awaji Island, Japan.

Manuscript Published: Wu R, Hu T, Rehemtulla A, Fearon ER, Cho KR. Preclinical Testing of PI3K/AKT/mTOR Signaling Inhibitors in a Mouse Model of Ovarian Endometrioid Adenocarcinoma. *Clin Cancer Res.* 2011 Sep 8. [Epub ahead of print], 17(23):7359-72, pdf attached (Appendix 1).

CONCLUSIONS:

We have generated mice that are transgenic for two different imaging reporters (*Rosa26*$^{LSL\text{-}Luc/+}$ and *Apoptosis*$^{LSL\text{-}Luc}$) that also carry floxed *Pten* and *Apc* alleles. Ovarian bursal injection of AdCre in these animals induces tumor formation and activation of the luciferase reporter alleles. We have shown that *Apc*$^{flox/flox}$*;Pten*$^{flox/flox}$*;Apoptosis*$^{LSL\text{-}Luc}$ mice can be used to image treatment-dependent induction of apoptosis. Efficacy of a targeted therapeutic agent (Akt inhibitor, Perifosine), alone and in combination with a standard chemotherapeutic agent (Cisplatin) was evaluated. Our studies revealed that combination therapy resulted in enhanced levels of apoptosis compared to either agent alone. Interestingly, although Cisplatin as a single agent was not able to induce apoptosis as robustly as Perifosine, in studies wherein tumor volumes were determined by MRI, Cisplatin was able to induce significantly enhanced tumor control compared to Perifosine as a single agent. These results suggest that Cisplatin, which is a DNA damaging agent, may induce tumor cell kill primarily through non-apoptotic mechanisms.

Based on the data we've collected, we believe that future studies of Cisplatin response should evaluate levels of non-apoptotic death (e.g autophagy) in addition to apoptosis. Autophagy is an alternative mode of cell demise, representing a self-cannibalization process that involves sequestration of cell structures in double-membraned organelles, called autophagosomes. The physiological role of autophagy is to remove long-lived proteins and damaged organelles, but when it is extensive, activated inappropriately or in cells which are unable to die by apoptosis, autophagy acts as an alternative cell-death pathway. It has been proposed that tumor cells in some conditions might employ autophagy as a mechanism to evade therapy-induced death. It has recently been shown that cisplatin-triggered autophagy partially protects primary renal tubular epithelial cells from concomitant induction of apoptotic cell death by the drug [Kaushal et. al., 2008]. Therefore, the ability of combined Cisplatin and Perifosine therapy to drive cells to undergo apoptosis may in the long run mechanistically delay

recurrence of OEA compared to Cisplatin alone. Validation of this hypothesis would require specifically designed studies.

REFERENCES:

Kaushal GP, Kaushal V, Herzog C, et al. Autophagy delays apoptosis in renal tubular epithelial cells in cisplatin cytotoxicity. Autophagy. 2008; 4: 710–2.

APPENDICES:

1. Reprint, R. Wu et al., *Clinical Cancer Research*, 17(23):7359-72, 2011, including Supplemental Figures and Figure Legends
2. Meeting Abstract submitted for plenary talk at the annual meeting of the Japanese Society for Advancement of Women's Imaging, September, 2011.
3. Copy of email from *Cell Cycle* Editor-in-Chief, Mikhail Blagosklonny, inviting contribution of "Feature" piece on *Clinical Cancer Research* paper.

BIBLIOGRAPHY OF PUBLICATIONS:

Wu R, Hu T, Rehemtulla A, Fearon ER, Cho KR. Preclinical Testing of PI3K/AKT/mTOR Signaling Inhibitors in a Mouse Model of Ovarian Endometrioid Adenocarcinoma. *Clin Cancer Res*. 2011 Sep 8. [Epub ahead of print], 17(23):7359-72, pdf attached (Appendix 1).

LIST OF PERSONNEL RECEIVING PAY FROM THE RESEARCH EFFORT:

Kathleen R. Cho (Initiating PI)
Yali Zhai (Research Investigator, Cho Laboratory)
Rong Wu (Research Assistant Professor, Cho Laboratory)
Rork Kuick (statistician)
Shamima Yeasmin (postdoctoral fellow)

Published OnlineFirst September 8, 2011; DOI:10.1158/1078-0432.CCR-11-1388

Clinical Cancer Research

Preclinical Testing of PI3K/AKT/mTOR Signaling Inhibitors in a Mouse Model of Ovarian Endometrioid Adenocarcinoma

Rong Wu, Tom C. Hu, Alnawaz Rehemtulla, et al.

Clin Cancer Res 2011;17:7359-7372. Published OnlineFirst September 8, 2011.

Published OnlineFirst September 8, 2011; DOI:10.1158/1078-0432.CCR-11-1388

Cancer Therapy: Preclinical

Clinical Cancer Research

Preclinical Testing of PI3K/AKT/mTOR Signaling Inhibitors in a Mouse Model of Ovarian Endometrioid Adenocarcinoma

Rong Wu[1], Tom C. Hu[1], Alnawaz Rehemtulla[2,4], Eric R. Fearon[1,3,4], and Kathleen R. Cho[1,3,4]

Abstract

Purpose: Genetically engineered mouse (GEM) models of ovarian cancer that closely recapitulate their human tumor counterparts may be invaluable tools for preclinical testing of novel therapeutics. We studied murine ovarian endometrioid adenocarcinomas (OEA) arising from conditional dysregulation of canonical WNT and PI3K/AKT/mTOR pathway signaling to investigate their response to conventional chemotherapeutic drugs and mTOR or AKT inhibitors.

Experimental Design: OEAs were induced by injection of adenovirus expressing Cre recombinase (AdCre) into the ovarian bursae of $Apc^{flox/flox}$;$Pten^{flox/flox}$ mice. Tumor-bearing mice or murine OEA-derived cell lines were treated with cisplatin and paclitaxel, mTOR inhibitor rapamycin, or AKT inhibitors API-2 or perifosine. Treatment effects were monitored *in vivo* by tumor volume and bioluminescence imaging, *in vitro* by WST-1 proliferation assays, and in OEA tissues and cells by immunoblotting and immunostaining for levels and phosphorylation status of PI3K/AKT/mTOR signaling pathway components.

Results: Murine OEAs developed within 3 weeks of AdCre injection and were not preceded by endometriosis. OEAs responded to cisplatin + paclitaxel, rapamycin, and AKT inhibitors *in vivo*. *In vitro* studies showed that response to mTOR and AKT inhibitors, but not conventional cytotoxic drugs, was dependent on the status of PI3K/AKT/mTOR signaling. AKT inhibition in APC^{-}/$PTEN^{-}$ tumor cells resulted in compensatory upregulation of ERK signaling.

Conclusions: The studies show the utility of this GEM model of ovarian cancer for preclinical testing of novel PI3K/AKT/mTOR signaling inhibitors and provide evidence for compensatory signaling, suggesting that multiple rather than single agent targeted therapy will be more efficacious for treating ovarian cancers with activated PI3K/AKT/mTOR signaling. *Clin Cancer Res; 17(23); 7359–72. ©2011 AACR.*

Introduction

More than two-thirds of women diagnosed with ovarian carcinoma present with advanced stage disease, and their overall 5-year survival is only 28% (1, 2). Although the initial response of ovarian carcinomas to standard therapy (surgical debulking and chemotherapy with platinum-based drugs and taxanes) is often excellent, relapse with drug-resistant cancer usually occurs and patients succumb to their disease. Over the last several years, much progress has been made in identifying hallmark genetic lesions associated with each major subtype of ovarian carcinoma. Novel therapeutics that target the signaling pathways dysregulated as a result of these molecular defects are being developed, with the hope that individualized therapeutic regimens based on the specific molecular defects present in a given patient's tumor could be used alone or in combination with existing cytotoxic agents to improve clinical outcome.

Surgical pathologists continue to use morphology-based schemes for classifying ovarian carcinomas (OvCas) based largely on their degree of resemblance to nonneoplastic epithelia in the female genital tract. However, mounting clinico-pathologic and molecular data have led Kurman and Shih to propose a new model in which OvCas are divided into 2 main categories—type I and type II (3–5). Type I OvCas are suggested to be low grade, relatively indolent and genetically stable tumors that arise from well-defined precursor lesions such as endometriosis or so-called borderline tumors, and frequently harbor somatic mutations that dysregulate certain cell signaling pathways (e.g., *KRAS*, *BRAF*, *CTNNB1*, *PTEN*). Type I OvCas include most endometrioid, clear cell, and mucinous carcinomas and low-grade serous carcinomas. In contrast, type II OvCas are proposed to be high-grade, biologically aggressive tumors from their outset, with a propensity for metastasis

Authors' Affiliations: Departments of [1]Pathology, [2]Radiation Oncology, [3]Internal Medicine; and [4]Comprehensive Cancer Center, The University of Michigan Medical School, Ann Arbor, Michigan

Note: Supplementary data for this article are available at Clinical Cancer Research Online (http://clincancerres.aacrjournals.org/).

Corresponding Author: Kathleen R. Cho, Department of Pathology, University of Michigan Medical School, 1506 BSRB, 109 Zina Pitcher, Ann Arbor, MI 48109. Phone: 734-764-1549; Fax: 734-647-7950; E-mail: kathcho@umich.edu

doi: 10.1158/1078-0432.CCR-11-1388

Published OnlineFirst September 8, 2011; DOI:10.1158/1078-0432.CCR-11-1388

Translational Relevance

Currently available therapies have improved survival for patients with advanced ovarian carcinoma, but many patients ultimately relapse and die from their cancer. There is great interest in designing new individualized therapeutic regimens based on the specific molecular defects present in a given patient's tumor. Although many drugs and drug combinations are potentially available, identification of the most efficacious of these remains a challenging process that cannot easily be conducted in women with the disease. We have shown the preclinical utility of a genetically engineered mouse model of ovarian carcinoma that closely resembles human endometrioid ovarian cancers with Wnt and PI3K/Akt/mTOR pathway defects for comparison of the activities of multiple drugs targeting activated PI3K/Akt/mTOR signaling. The data suggest the mouse model strategy described here should help accelerate the transition of the most promising new therapies from the laboratory into clinical trials.

from small-volume primary lesions. Most type II OvCas are high-grade serous carcinomas, virtually all of which harbor mutant *TP53* alleles (6).

Genetic alterations that dysregulate the canonical Wnt (i.e., Wnt/β-catenin/Tcf) and PI3K/Akt/mTOR signaling pathways often occur together in human ovarian endometrioid adenocarcinoma (OEA; refs. 7, 8). Given substantial overlap in the molecular features (gene expression and mutational profiles) of tumors diagnosed as high-grade OEAs, with high-grade serous carcinomas (7), some pathologists default the majority of gland-forming or near-solid cytologically high-grade carcinomas to the serous category, and consider true high-grade OEAs to be rare or nonexistent (9). If only low-grade (prototypical type I) OEAs are considered, the majority have mutations predicted to dysregulate canonical Wnt and/or PI3K/Akt/mTOR signaling and *TP53* is usually wild type. Loss of function mutations in *ARID1A* (which encodes the AT-rich interactive domain-containing protein 1A) have also been recently reported in 30% of OEAs (10). Given the frequency with which Wnt and PI3K/Akt/mTOR signaling is activated in OEAs, drugs that target these pathways might prove to be particularly useful for treating patients with advanced-stage disease or in the adjuvant setting for patients with OEA who might be at risk of recurrence. Given our limited ability to exhaustively test multiple drug combinations, doses, and schedules in clinical trials, it is anticipated that animal models which closely mimic their human disease counterparts will provide an invaluable tool for the identification of multidrug regimens with greatest promise for efficacy in humans.

We previously described a murine model of (type I) OEA based on conditional inactivation of the *Apc* and *Pten* tumor suppressor genes following injection of adenovirus expressing Cre recombinase (AdCre) into the ovarian bursae of $Apc^{flox/flox};Pten^{flox/flox}$ mice (7). Several characteristics of this mouse model suggest its relevance and tractability for testing novel therapeutic approaches. First, complicated breeding schemes are not needed to generate mice with the appropriate genotype once a breeding colony has been established. Second, tumors invariably arise within a few weeks following AdCre injection, and recapitulate the morphology and gene expression pattern of human OEAs with comparable signaling pathway defects. Third, tumors arise in the ovary and in immunologically intact animals, so possible effects of the tumor microenvironment on therapeutic response can be assessed. Finally, similar to women with advanced ovarian cancer, 3 quarters of the mice develop hemorrhagic ascites, and nearly one quarter acquire overt peritoneal dissemination. To show this model's utility for preclinical testing of novel therapeutics targeting the PI3K/Akt/mTOR signaling pathway, we pursued proof-of-principle studies showing the response of murine OEAs to conventional chemotherapeutic drugs (cisplatin and paclitaxel) and mTOR and AKT inhibitors *in vitro* and *in vivo*. In addition, we show the application of a Cre-inducible luciferase reporter allele for longitudinal *in vivo* monitoring of tumor development and drug response in the mice.

Materials and Methods

Mouse strains and tumor induction

$Apc^{flox/flox};Pten^{flox/flox}$ mice and ovarian bursal delivery of replication-incompetent recombinant AdCre have been described previously in detail (7). Briefly, Cre-mediated recombination in these animals results in a frameshift mutation at *Apc* codon 580 (11), and the deletion of exons 4 and 5 of *Pten* (12). For tumor induction, 5×10^7 plaque-forming units of AdCre (purchased from the University of Michigan's Vector Core) with 0.1% Evans Blue (Sigma-Aldrich Inc.) were injected into the right ovarian bursal cavities of 2- to 5-month-old female mice. In each mouse, the left ovarian bursa was not injected and served as control. Six weeks following AdCre injection, cohorts of mice were randomly assigned to drug treatment or vehicle control groups unless otherwise specified. Animals were euthanized by CO_2 asphyxiation following 3 to 4 weeks of drug treatment. All animal studies were done under a protocol approved by the University of Michigan's University Committee on Use and Care of Animals.

Cell lines

W2671T and W2830T cell lines were generated from $APC^{-}/PTEN^{-}$ murine ovarian tumors. Briefly, fresh ovarian tumor tissues were mechanically minced with sterile scalpels and further digested at 37°C with 0.05% Trypsin-EDTA for 20 minutes. Cells were cultured for 5 passages in Dulbecco's Modified Eagle's Medium (DMEM) containing 10% FBS/1% penicillin/streptomycin (P/S)/1% Insulin-transferrin-selenium (Invitrogen) in an incubator with 3% O_2/5% CO_2 (Model NAPCO 8000WJ, Thermal Scientific). Cells were maintained in DMEM supplemented with

Published OnlineFirst September 8, 2011; DOI:10.1158/1078-0432.CCR-11-1388

10% FBS/1% P/S in a standard 5% CO_2 incubator (Model 3307, Thermo Scientific). ID8 cells (spontaneously transformed ovarian surface epithelial cells from a C57B/L6 mouse) were obtained from KF Roby (University of Kansas Medical Center; ref. 13). The human OEA-derived cell line TOV-112D and ovarian carcinoma cell line A2780 were obtained from the American Type Culture Collection. TOV-112D cells harbor an activating (S37A) *CTNNB1* mutation (14), but lack known PI3K/AKT/mTOR pathway defects. A2780 has biallelic inactivation of *PTEN* (9bp deletion in exon 5 and 37bp deletion in exon 8) but lacks known canonical Wnt pathway defects (15). To generate human ovarian carcinoma cells with dysregulation of both PI3K/Akt/mTOR and Wnt signaling, we transduced A2780 cells with a mutant (oncogenic) form of β-catenin (S33Y) by infecting cells with S33Y β-catenin–expressing retroviruses or control (PGS-CMV-CITE-neo; ref. 16).

Drugs and treatment in mice

Rapamycin (LC Laboratories) was reconstituted in 100% ethanol at 10 mg/mL, stored at −30°C and diluted in 5% Tween-80 and 5% PEG-400 before injection. Rapamycin was injected i.p. at concentrations of 4 mg/kg ($n = 5$) or 1 mg/kg ($n = 8$) in a final volume of 100 μL, 3 times weekly for 4 weeks. API-2 (Calbiochem) in 5% dimethyl sulfoxide (DMSO) was injected i.p. at a dose of 1 mg/kg in 100 μL daily for 3 to 4 weeks. Control mice were treated with 5% DMSO alone. Perifosine in 0.9% NaCl (Cayman Chemical) was given by oral gavage (125 mg/kg, twice weekly) for 4 weeks. The control group was administered 0.9% NaCl orally in parallel. Cisplatin (LC Laboratories) in 0.9% NaCl (5 mg/kg) and paclitaxel (LC Laboratories) in 5% DMSO (20 mg/kg) were administered via i.p. injection, once a week for 4 weeks. Cisplatin and paclitaxel were administered on the same day, with paclitaxel being given 20 minutes after cisplatin. Control mice were given 0.9% NaCl first, then 5% DMSO.

WST-1 cell proliferation assay

WST-1 assays for cell proliferation were done per the manufacturer's instructions (Roche Applied Science). Briefly, 1×10^4 to 2×10^4 cells were plated in each well of 96-well plates and cultured overnight. After addition of drugs, cells were incubated for another 24 hours. Cell proliferation reagent (10 μL per well) was then added and cells were incubated for another 2 to 3 hours. Absorbance of the samples at 450 and 600 nm was measured with a 96-well spectrophotometric plate reader (SpectraMax 190, Molecular Devices). Effects of drug treatments on cell proliferation were evaluated using 1-way ANOVA (GraphPad Prism, version 5.01 GraphPad Software, Inc.).

Immunoblotting

Cultured cells were treated with rapamycin (0.01–100 nmol/L) or API-2 (40 μmol/L) for up to 24 hours or with perifosine (40–80 μmol/L) for 2 hours. Whole cell protein lysates were then prepared in (radioimmunoprecipitation assay (RIPA) buffer containing Complete Protease Inhibitor Cocktail Tablets (Roche) and Phosphatase inhibitor cocktails (Sigma). Immunoblotting was done using standard protocols. Total protein lysates (30–50 μg) were separated on NuPage 4% to 12% Bis-Tris precast gels (Invitrogen) and then transferred to Immobilon-P membranes (Millipore). Antibody complexes were detected with enhanced chemiluminescent reagents (PerkinElmer) and exposed to HyBlot CL film (Denville Scientific Inc.).

Histopathology and immunohistochemistry

After drug treatment, all mice were euthanized and examined at necropsy for gross organ abnormalities. The genital tract and other major organs were collected, fixed in 10% (v/v) buffered formalin, embedded in paraffin, and processed for staining with hematoxylin and eosin (H&E). Histopathologic evaluation of tumor and other tissues was done by a surgical pathologist with expertise in gynecologic cancer diagnosis (K.R. Cho). Immunohistochemical (IHC) staining was done on formalin-fixed, paraffin-embedded tissues or frozen sections using standard methods. For mouse primary antibodies, mouse on mouse kit (M.O.M., Vector Laboratories Inc.) was used to reduce nonspecific staining per the manufacturer's instructions. Immunofluorescence staining was carried out as previously described (14). Briefly, cells were grown in chamber slides for 2 days, then fixed with 4% paraformaldehyde for 20 minutes and permeabilized with 1% goat serum/0.5% Triton X-100/PBS for 15 minutes at room temperature. After washing with PBS, slides were blocked with 2% goat serum/0.2% TritonX-100/PBS for 60 minutes. Cells were incubated with primary antibody at 4°C overnight. After washing with PBS, cells were incubated with Alexa 594 Red-conjugated secondary antibody at a dilution of 1:1,000 for 60 minutes at room temperature. Slides were washed with PBS and then counterstained with Hoechst (1:1,000) for 5 minutes. Prolong Gold antifade reagent (Fisher) was used to mount the coverslips.

Antibodies

The following primary antibodies were used for IHC or immunofluorescent staining: Mouse anti–β-catenin (Transduction Laboratories); Mouse anti–α-inhibin (Serotac Ltd.); Rat anti-cytokeratin 8 (CK8, #TROMA 1, Developmental Studies Hybridoma Bank, University of Iowa); Rat anti-Ki67 (clone TEC-3, Dako); Rabbit anti-pten (clone 138G6, Cell Signaling, #9559); Rabbit anti-cleaved caspase-3 (Asp175) Cell Signaling, #9661); Rabbit anti-phospho-S6 Ribosomal Protein (Ser235/236; Cell Signaling, #4857); and mouse anti-CD10 (Novocastra, #NCL-CD-270). Antibodies used for immunoblotting were: Rabbit anti-phospho-AKT (Ser473; Cell Signaling, #4060); Rabbit anti-AKT (Cell Signaling, #9272); Mouse anti-phospho-ERK (E-4; Santa Cruz, #7383); Rabbit anti-ERK1/2 (Cell Signaling, #9102); Rabbit anti-phospho-S6 Ribosomal Protein (Ser235/236; Cell Signaling, #4857); Mouse anti-S6 Ribosomal Protein (Cell Signaling, #2317); Rabbit anti phospho-p70 S6 (Thr389) kinase (Cell Signaling, #9205); Rabbit anti-p70 S6 kinase (Santa Cruz, #SC-

Published OnlineFirst September 8, 2011; DOI:10.1158/1078-0432.CCR-11-1388

230); Rabbit anti-phospho-4E-BP1 (Thr70; Cell Signaling, #9455); Rabbit anti-phospho-4E-BP1 (Thr37/46; Cell Signaling, #2855); Rabbit anti-4E-BP1 (Cell signaling, #9644); Mouse anti-active β-catenin (Clone 8E7, Millipore); Rabbit anti-phospho-GSK3β (Ser9; Cell Signaling, #9323); and Rabbit anti-GSK3β (Cell Signaling, #9315).

In vivo bioluminescence imaging

The mouse luciferase reporter strain *Rosa26*$^{L\text{-}S\text{-}L\text{-}Luc/+}$ (17) was purchased from the Jackson Laboratory (stock #005125). Luciferase expression in the mouse ovarian surface epithelium was induced by ovarian intrabursal injection of AdCre. Mice were imaged using an IVIS Image System 200 Series (Xenogen Corporation). During the imaging procedure, mice were anaesthetized with a constant flow of 1.5% isoflurane from the IVIS manifold and then administered a single i.p. dose of D-luciferin (150 mg/kg, Biosynth International, Inc.) in a volume of 100 μL in normal saline. Image acquisition was initiated approximately 10 minutes after injection of D-luciferin. The bioluminescence signals (photons/s) emitted from the mice were collected using sequential mode until reaching peak values and analyzed by LivingImage 3.0 software (Xenogen Corporation). For studies of tumor-bearing animals, *Rosa26*$^{L\text{-}S\text{-}L\text{-}Luc/+}$ and *Apc*$^{flox/flox}$;*Pten*$^{flox/flox}$ mice were crossed to generate *Apc*$^{flox/flox}$;*Pten*$^{flox/flox}$;*Rosa26*$^{L\text{-}S\text{-}L\text{-}luc/+}$ mice. After baseline imaging 6 weeks after AdCre infection, mice were treated with either drug or vehicle. Treated mice were then reimaged at weekly intervals for 4 weeks. For each animal, bioluminescence was normalized to its baseline (before treatment, 0 week) and signals were adjusted to the same color scale for the entire time course.

Results

Temporal analysis of ovarian murine tumor development following AdCre injection

Our previous studies have shown that mice-bearing APC^{-}/PTEN^{-} tumors survive 11 to 12 weeks on average (range 7–19 weeks) after injection of AdCre. To assess the possible value of this model for studying effects of chemoprevention or early intervention, we sought to define the earliest time point at which OEAs or precursor lesions could be detected. Cohorts of *Apc*$^{flox/flox}$;*Pten*$^{flox/flox}$ mice (total, $n = 43$) were evaluated weekly from 1 to 6 weeks after ovarian bursal AdCre injection. Mice were euthanized and their genital tracts evaluated for gross and microscopic lesions; data are summarized in Table 1. No gross or microscopic lesions were detectable in any of the mice examined at 1 ($n = 2$) or 2 ($n = 8$) weeks after AdCre injection. In 6 of 10 mice euthanized after 3 weeks, microscopic dysplastic lesions were found exclusively in the injected (right) ovaries (Fig. 1A and B). Multifocal aggregates of epithelial cells (tumorlets), morphologically indistinguishable from those seen in well-established tumors, were present on the ovarian surface. On the basis of IHC staining, cells in the surface tumorlets were cytokeratin 8-positive (Fig. 1C) and α-inhibin-negative (Fig. 1D), consistent with epithelial differentiation. As expected, the tumor cells also showed strong nuclear expression of β-catenin (Fig. 1E) and absence of PTEN expression (Fig. 1F). In 13 mice euthanized 6 weeks post-AdCre injection, 2 had microscopic ovarian tumorlets and 11 had grossly visible, small ovarian tumors (Fig. 1G); none had developed ascites or peritoneal metastasis. Microscopically, the 6-week tumors showed areas of overt glandular differentiation (Fig. 1H) admixed with more poorly differentiated and spindle cell areas as observed in the more advanced tumors we described previously (7).

Table 1. Ovarian tumor development following AdCre injection

Week	Number of mice	Microscopic tumor	Macroscopic tumor	% with tumor
1	2	0	0	0
2	8	0	0	0
3	10	6	0	60
4	7	6	0	85.7
5	3	3	0	100
6	13	2	11	100

Development of APC^{-}/PTEN^{-} murine ovarian tumors is not preceded by endometriosis

A substantial proportion of human ovarian carcinomas with endometrioid or clear cell differentiation are believed to arise from endometriosis (18). Notably, we did not observe endometriosis-like lesions in any of the 43 *Apc*$^{flox/flox}$;*Pten*$^{flox/flox}$ mice evaluated 1 to 6 weeks following AdCre injection or, in our previous study, in mice with well-established APC^{-}/PTEN^{-} tumors (7). After ovarian bursal injection of AdCre, groups of mice where only the *Apc* (*Apc*$^{flox/flox}$) or *Pten* (*Pten*$^{flox/flox}$) genes were individually inactivated were monitored for 12 to 13 months for tumor development. No ovarian epithelial tumors were found in either group, though benign endometrial-type glands and stroma morphologically similar to endometriosis were observed at the end of the monitoring period in the injected (right) ovaries in 9 of 49 *Apc*$^{flox/flox}$ mice. Similar lesions were identified in the uninjected (left) ovaries of 6 mice (Fig. 2A and B). In *Pten*$^{flox/flox}$ control mice ($n = 47$), endometriosis was observed in one AdCre injected ovary. We did not observe tumor formation or endometriosis lesions in any of 24 C57BL/6J mice monitored from 3 to 13 months following ovarian bursal AdCre injection. As expected for endometriosis, IHC staining showed strong CK8 positivity in the glandular epithelium and scattered CD10-positive cells in the adjacent endometriotic stroma (Fig. 2C and D). Expression of α-inhibin was weak in the stroma relative to the granulosa cells in the ovarian follicles (Fig. 2E). Importantly, the glandular epithelium showed exclusively membranous staining for β-catenin, indicating absence of Cre-mediated inactivation of

Published OnlineFirst September 8, 2011; DOI:10.1158/1078-0432.CCR-11-1388

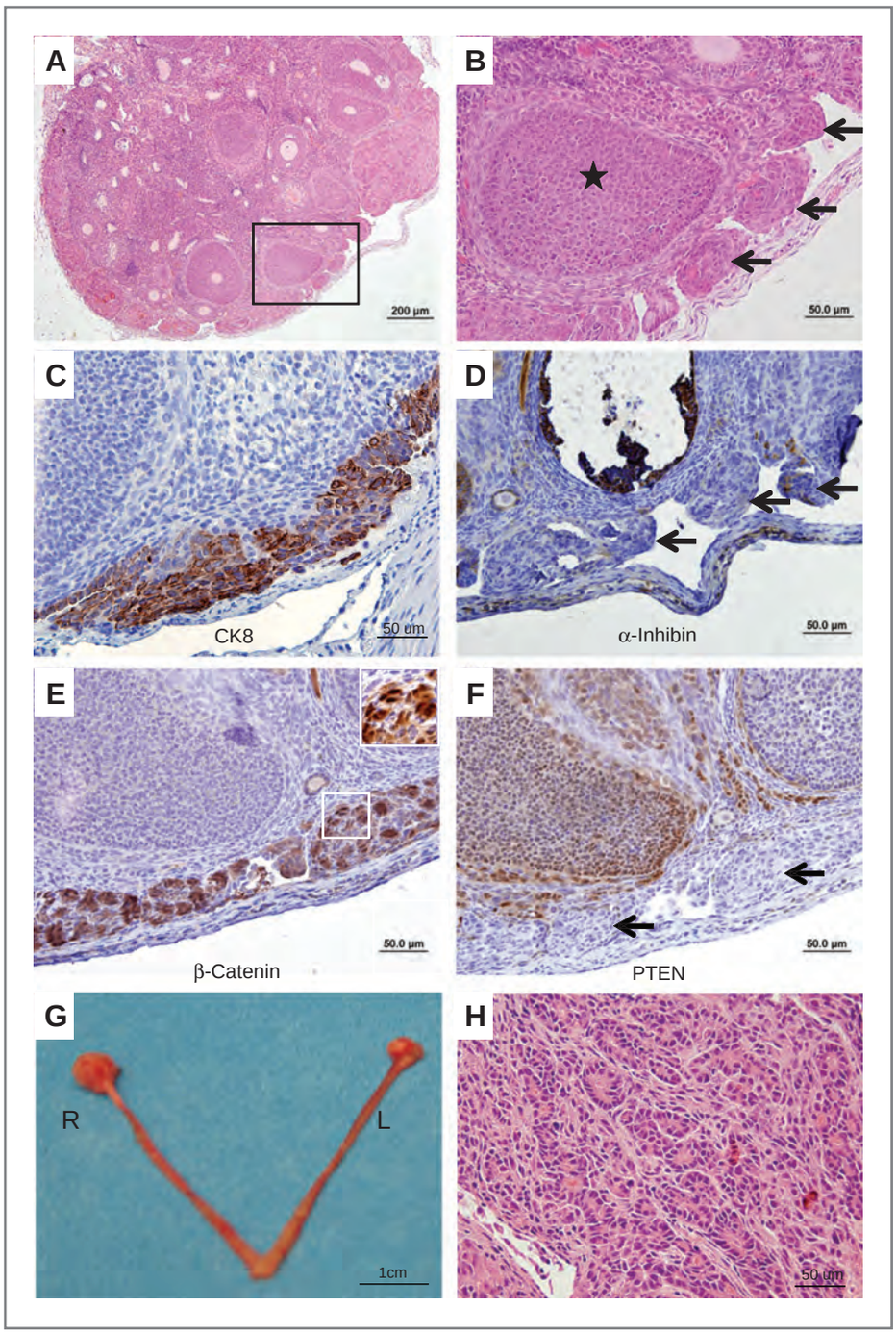

Figure 1. Murine OEA-like tumors arise within 3 weeks of ovarian bursal AdCre injection in *Apc*$^{flox/flox}$; *Pten*$^{flox/flox}$ mice. A, low magnification photomicrograph of H&E stained section from right ovary 3 weeks after AdCre injection showing multifocal tumorlets on the ovarian surface. B, high magnification photomicrograph of the boxed area in A showing tumorlets (arrows) and ovarian follicle (star). Tissue sections were IHC stained for cytokeratin 8 (C); α-inhibin (D); β-catenin (E); and PTEN (F). Cells in the surface tumorlets are positive for cytokeratin 8 and show strong nuclear staining for β-catenin. The tumor cells are negative for α-inhibin and PTEN (arrows indicate tumorlets). G, gross photograph of upper genital tract 6 weeks after AdCre injection of right ovarian bursa shows modestly enlarged right (R) ovary relative to the control left (L) ovary. H, photomicrograph of H&E stained section from ovarian tumor present 6 weeks after AdCre injection. Areas of overt glandular differentiation are admixed with poorly differentiated and spindle cell areas.

Apc, even in the AdCre-injected ovaries (Fig. 2F). This finding, in addition to our observation of endometriosis-like lesions in the uninjected and injected ovaries, suggests, but does not definitively prove, that the development of endometriosis in a subset of the mice is not dependent on Cre-mediated inactivation of *Apc* or *Pten*, but may instead reflect a background rate of endometriosis development that varies to some degree with the genetic background of the mice studied.

Status of PI3K/AKT/mTOR signaling in murine ovarian cancer cells determines response to AKT and mTOR inhibitors, but not to conventional cytotoxic drugs

The PI3K/AKT/mTOR signaling pathway plays an important role in the regulation of cell growth, proliferation, and survival by controlling the phosphorylation of several translation factors. We first wished to test effects of selected PI3K/AKT/mTOR pathway-targeted therapies and conventional cytotoxic agents on murine tumor cell

Published OnlineFirst September 8, 2011; DOI:10.1158/1078-0432.CCR-11-1388

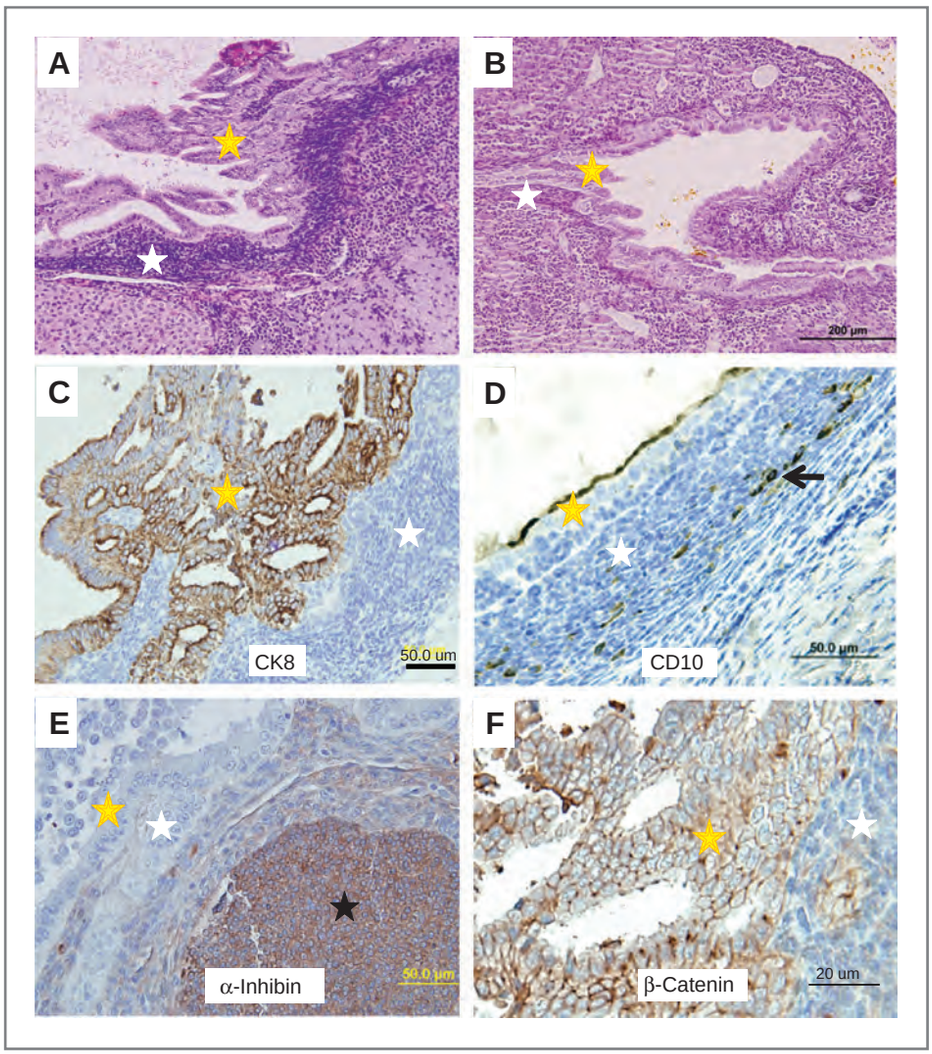

Figure 2. Endometriosis-like lesions are present in the ovaries of *Apc*$^{flox/flox}$ mice. Photomicrographs of H&E stained sections from the right (A) and left (B) ovaries of *Apc*$^{flox/flox}$ mice 12 months after AdCre injection showing endometriosis-like lesions with endometrial-type glands (yellow stars) and adjacent stroma (white stars). Tissue sections with endometriosis were IHC stained for cytokeratin 8 (C), CD10 (D), α-inhibin (E), and β-catenin (F). The glandular epithelium (yellow stars) is strongly positive for cytokeratin 8, negative for α-inhibin, and shows membranous staining for β-catenin. The adjacent stroma shows focal CD10 positivity (black arrow) and is only weakly positive for α-inhibin compared with granulosa cells in the ovarian follicle (black star).

proliferation *in vitro*. WST-1 proliferation assays were done using 3 transformed murine ovarian surface epithelial cell lines. The W2671T and W2830T cell lines were established in our laboratory following primary culture of murine OEAs induced by AdCre injection in *Apc*$^{flox/flox}$; *Pten*$^{flox/flox}$ mice. These cells show epithelial-like cobblestone morphology in culture (Supplementary Fig. S1A and B). The cells are cytokeratin 8- (Supplementary Fig. S1C) and E-cadherin-positive, and vimentin-negative (Supplementary Fig. S1D) based on immunofluorescent staining. ID8 cells, a spontaneously transformed mouse ovarian surface epithelial cell line lacking known PI3K/AKT/mTOR and canonical WNT pathway defects, were also used for our studies (13). Cells were incubated with different doses of drugs for 24 hours, and data were normalized to vehicle treatment. W2671T cells displayed profound dose-dependent growth inhibition in response to rapamycin, cisplatin, and paclitaxel (Fig. 3A–C). More modest inhibitory effects were observed with perifosine, a synthetic alkyl phospho-lipid that targets cell membranes and inhibits PKB-mediated AKT activation (Fig. 3D; ref. 19). Statistically significant growth inhibition was observed in W2671T at the highest (40 μmol/L) perifosine concentration. In contrast, ID8 cells were sensitive to cisplatin and paclitaxel but showed minimal response to rapamycin, and no response to perifosine, even at the highest concentrations. These results confirm differential sensitivity to drugs that target PI3K/AKT/mTOR signaling in murine ovarian cancer cells, depending on the presence or absence of PI3K/AKT/mTOR pathway defects in the cells.

Characterization of PI3K/AKT/mTOR signaling pathway regulation in murine and human ovarian cancer cells after rapamycin treatment *in vitro*

The serine/threonine protein kinase mTOR exists in 2 functional complexes, mTORC1 and mTORC2. mTORC1 is a major regulator of cell growth, containing mTOR, raptor, and mLST8. mTORC1 phosphorylates ribosomal protein S6 kinase beta-1 (S6K1) at Thr389, which is necessary for

Published OnlineFirst September 8, 2011; DOI:10.1158/1078-0432.CCR-11-1388

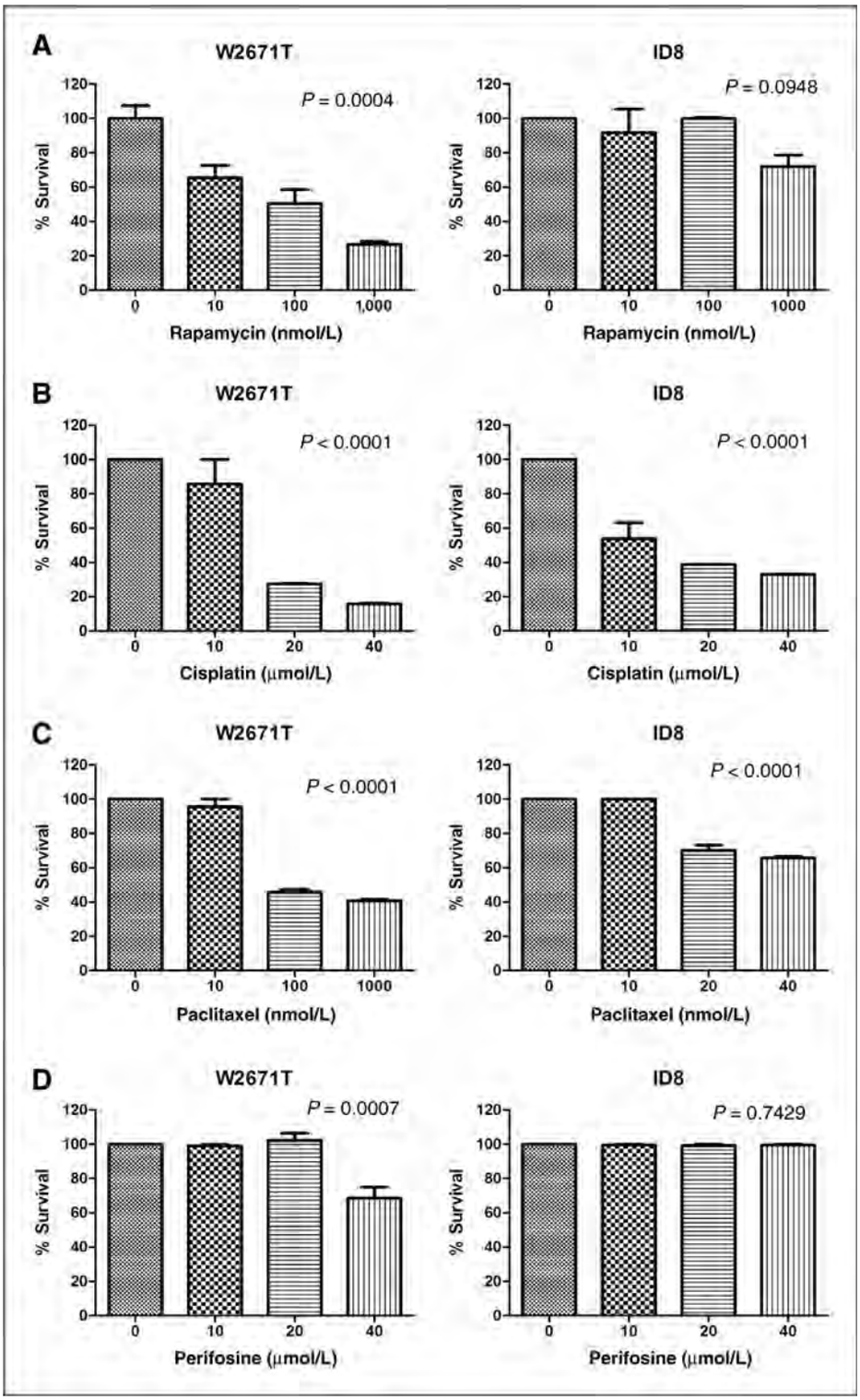

Figure 3. Status of PI3K/AKT/mTOR signaling in murine ovarian cancer cells determines response to Akt and mTOR inhibitors, but not to conventional cytotoxic drugs. Growth inhibitory effects of rapamycin (A), cisplatin (B), paclitaxel (C), and perifosine (D) were evaluated in W2671T, W2830T, and ID8 cells *in vitro*. After exposure to indicated drugs or controls for 24 hours, cell viability was measured with WST-1 reagent. Proportional viability (%) was calculated by comparing the drugs with vehicle controls whose viability was assumed to be 100%. Values represent the average of 3 independent assays done in duplicate, expressed as means ± SD. Differences between control and treated cells were analyzed by 1-way ANOVA.

activation and phosphorylation of the eukaryotic translation initiation factor 4E-binding protein 1 (4E-BP1). Phosphorylation of 4E-BP1 blocks its binding to eIF4E and results in increased translation of capped mRNAs. Phosphorylated S6K1 further phosphorylates ribosomal protein S6 (S6) to promote ribosome biogenesis. Rapamycin suppresses both cell proliferation and cell growth through inhibition of mTORC1 (20, 21). mTORC2, comprised of

Published OnlineFirst September 8, 2011; DOI:10.1158/1078-0432.CCR-11-1388

mTOR, Rictor, mSin1, and mLST8, is relatively resistant to rapamycin. mTORC2 regulates activation of Akt, and mTORC2 activity is stimulated by growth factors such as insulin and insulin growth factor-1 (IGF-1).

To further characterize the time and dose-dependent downstream effects of drug-target interactions *in vitro*, the status of several PI3K/AKT/mTOR signaling pathway components was evaluated in 2 murine OEA-derived cell lines (W2671T, W2830T) before and after rapamycin treatment. As expected, in the absence of drug treatment, W2671T and W2830T cells exhibited constitutive phosphorylation (p) of AKT (Ser473), S6K1 (Thr389), and S6 (Ser235/236). In contrast, there was no or very low level expression of pAKT, pS6K1, and pS6 in ID8 cells, which lack known PI3K/AKT/mTOR and Wnt signaling pathway defects (Fig. 4A). Levels of p4E-BP1 were similarly low in all 3 cell lines. Several investigators have reported that 100 to 1,000 nmol/L rapamycin treatment can inhibit activation of endogenous mTOR (22, 23). Treatment of W2671T and W2830T cells with 100 nmol/L rapamycin more than a 24-hour time course showed complete loss of pS6K1 by the 0.5 hours time point and loss of pS6 between 0.5 and 4 hours. The timing of pAKT loss in reponse to rapamycin varied between the 2 lines, but pAKT was undetectable in both lines by the 24 hours time point (Fig. 4B). Levels of p4E-BP1 were largely unchanged by rapamycin treatment, in keeping with recent reports that combined inhibition of Akt and Erk signaling is required to suppress 4E-BP1 phosphorylation (24). To determine the minimal concentration of rapamycin needed to abolish pS6K1 and pS6 expression in our murine APC^{-}/PTEN^{-} OEA cells, W2671T cells were treated for 2 hours with doses of rapamycin ranging from 0.01 to 100 nmol/L. Expression of pS6K1 and pS6 was virtually undetectable with rapamycin concentrations as

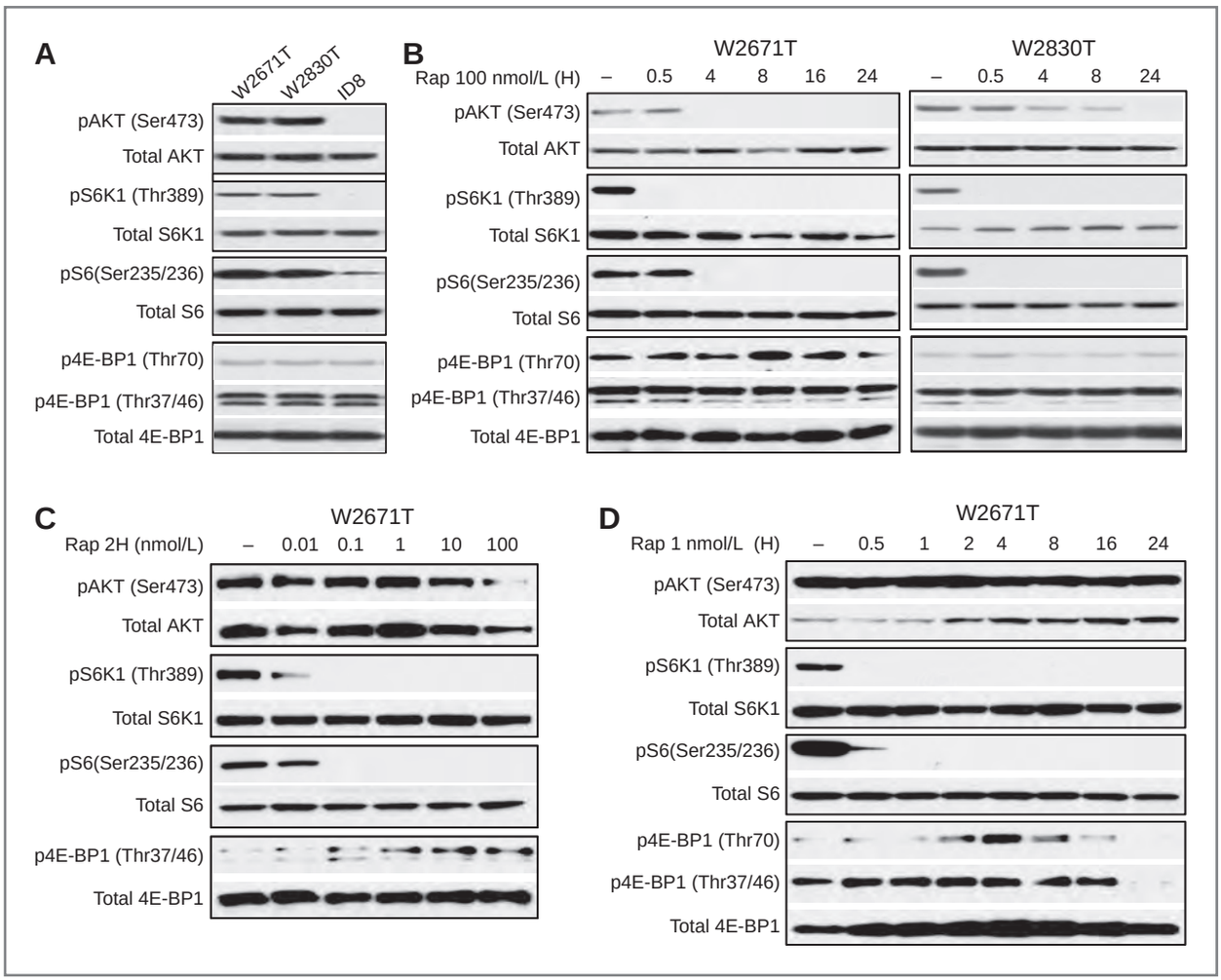

Figure 4. Characterization of PI3K/AKT/mTOR signaling pathway regulation in murine ovarian cancer cells after treatment with mTOR or Akt inhibitors. Immunoblots showing endogenous levels of phosphorylated and total Akt, S6K1, S6, and 4E-BP1 in W2671T, W2830T, and ID8 cells (A). B, time course of high dose (100 nmol/L) rapamycin treatment of W2671T and W2830T cell lines. Phosphorylated and total Akt, S6K1, S6, and 4E-BP1 are shown. C, dose-dependent effect of rapamycin (0.01–100 nmol/L) on phosphorylation of Akt, S6K1, S6, and 4E-BP1 after exposure to rapamycin for 2 hours in W2671T. D, time course of low dose (1 nmol/L) rapamycin treatment of W2671T cells. Phosphorylated and total Akt, S6K1, S6, and 4E-BP1 are shown.

Published OnlineFirst September 8, 2011; DOI:10.1158/1078-0432.CCR-11-1388

low as 0.1 nmol/L (Fig. 4C). In contrast to W2671T cells treated with 100 nmol/L rapamycin (Fig. 4B), cells treated with 1 nmol/L of rapamycin showed no change in AKT phosphorylation more than a 24-hour time course (Fig. 4D). At both the 1 nmol/L and 100 nmol/L rapamycin doses, early and sustained decreases in phosphorylation of both S6K1 and S6 were observed (Fig. 4B and D). These findings suggest that, in our model system, low doses of rapamycin inhibit only mTORC1, while higher doses are able to inhibit both mTORC1 and mTORC2. Interestingly, p4E-BP1 (Thr70) was elevated after 2 hours of low-dose (1 nmol/L) rapamycin treatment, peaked at 4 hours, then gradually decreased and was completely inhibited at 24 hours (Fig. 4D). p4E-BP1 (Thr37/46), the form with phosphorylation of the priming sites required for Thr70 phosphorylation, was increased between 0.5 and 16 hours and was nearly undetectable at 24 hours (Fig. 4D). These changes in p4E-BP1 levels were not observed with the high dose (100 nmol/L) of rapamycin (Fig. 4B).

We wished to determine whether rapamycin treatment yielded comparable effects in human ovarian cancer cells with canonical Wnt and/or PI3K/Akt/mTOR pathway defects. The TOV-112D cell line was derived from a human OEA and harbors mutant *CTNNB1* and wild-type *PTEN* alleles (14). As expected, TOV-112D cells expressed substantial levels of transcriptionally active β-catenin (dephosphorylated on Ser37 or Thr41) that were not affected by rapamycin. pAkt was undetectable at baseline and after 2 hours of treatment with rapamycin doses between 0.1 and 100 nmol/L (Supplementary Fig. S2A), and remained undetectable after 24 hours of treatment (data not shown). Expression of pS6K1 and pS6 was inhibited by treatment with rapamycin concentrations as low as 0.1 to 1.0 nmol/L. p(Ser9)GSK3β was modestly inhibited by 1 to 100 nmol/L rapamycin, consistent with GSK3β as a downstream target of Akt in cells with intact PI3K/Akt/mTOR signaling. A2780 ovarian carcinoma cells have biallelic inactivation of *PTEN* (15). These cells were transduced with a mutant (S33Y) form of β-catenin to generate a human ovarian cancer cell line with dysregulation of both Wnt and PI3K/AKT/mTOR signaling. As expected, and in contrast to TOV-112D cells, A2780 cells with and without mutant β-catenin show elevated pAkt at baseline (Supplementary Fig. S2B). Effects of rapamycin on PI3K/Akt/mTOR pathway components were largely similar in the presence and absence of mutant β-catenin, indicating Wnt pathway defects do not significantly alter effects of rapamycin in ovarian cancer cells with dysregulated PI3K/Akt/mTOR signaling. Our data are also consistent with previous reports that phosphorylation of S6K and S6 is not regulated by β-catenin (25).

Growth of APC^{-}/PTEN^{-} murine OEAs is inhibited *in vivo* by conventional chemotherapy and drugs targeting activated PI3K/AKT/mTOR signaling

The response of mouse OEAs to AKT and/or mTOR inhibitors *in vivo* would help show the model's potential utility for testing novel drugs targeting activated PI3K/AKT/mTOR signaling. Because clinical trials in ovarian cancer patients would likely compare the activity of targeted agents to that of conventional cytotoxic chemotherapy, it would also be useful to know whether the murine APC^{-}/PTEN^{-} tumors respond to cisplatin/paclitaxel *in vivo*. We therefore tested tumor-bearing mice for response to rapamycin, a first-generation mTOR inhibitor that directly binds mTORC1, a downstream effector of activated AKT. Tumor response to conventional combination therapy with cisplatin and paclitaxel and 2 mechanistically distinct AKT inhibitors (API-2 and perifosine) was also evaluated. API-2 (Akt/protein kinase B signaling inhibitor-2), also known as triciribine, is a cell-permeable tricyclic nucleoside that selectively inhibits the cellular phosphorylation/activation of AKT (26), while perifosine targets cell membranes and inhibits PKB-mediated AKT activation (19). Perifosine has also been shown to facilitate degradation of mTOR signaling pathway components including mTOR, raptor, rictor, S6K, and 4E-BP1 (27).

For these experiments, AdCre was injected into the right ovarian bursa of *Apc*$^{flox/flox}$;*Pten*$^{flox/flox}$ mice and drug (or vehicle) treatment was initiated after 6 weeks, when all of the mice were expected to have developed at least small tumors based on the studies described above. Data collected after 4 weeks of treatment with rapamycin (2 doses), API-2, perifosine and cisplatin/paclitaxel are shown in Fig. 5A–D, respectively. Treatment with each regimen, including both low (1 mg/kg) and high (4 mg/kg) doses of rapamycin, resulted in statistically significant inhibition of tumor growth more than 4 weeks based on measurements of tumor volume at necropsy. Microscopic analysis of H&E stained sections showed that residual drug-treated tumors were morphologically similar to vehicle-treated tumors (data not shown). None of the drug-treated animals developed liver metastases during the treatment period (compared with 3 of the vehicle-treated mice), and only 2 of 36 (6%) drug-treated mice (both in the low-dose rapamycin group) developed ascites, compared with 12 of 33 (36%) vehicle-treated mice. These data are summarized in Table 2.

Effects of drug treatment on cell proliferation in the residual ovarian tumors were evaluated by IHC staining for Ki-67 in tumor tissue sections. The Ki-67 index was defined as the percentage of Ki-67 positive cells in the most cellular areas of tumor. Data from two 400× fields were collected and averaged. The Ki-67 index was significantly reduced in rapamycin-treated tumors ($n = 12$) compared with vehicle-treated tumors ($n = 6$) in control mice ($28.03 \pm 3.27\%$ vs. $41.84 \pm 4.82\%$, $P = 0.0418$). The Ki-67 index was also lower in perifosine-treated tumors relative to vehicle-treated controls, but the difference did not achieve statistical significance ($31.49 \pm 1.61\%$ vs. $46.15 \pm 6.61\%$, $P = 0.097$). API-2 had no appreciable effect on the Ki-67 index ($48.80 \pm 5.41\%$ vs. $42.21 \pm 4.47\%$, $P = .3747$). Apoptosis in rapamycin versus vehicle-treated tumors was evaluated by IHC staining for the active form of caspase-3, cleaved caspase-3 (CC3), using an antibody that recognizes the p20/p17 subunit in the cytoplasm of apoptotic cells. Only rare positive cells were identified in tissue

Published OnlineFirst September 8, 2011; DOI:10.1158/1078-0432.CCR-11-1388

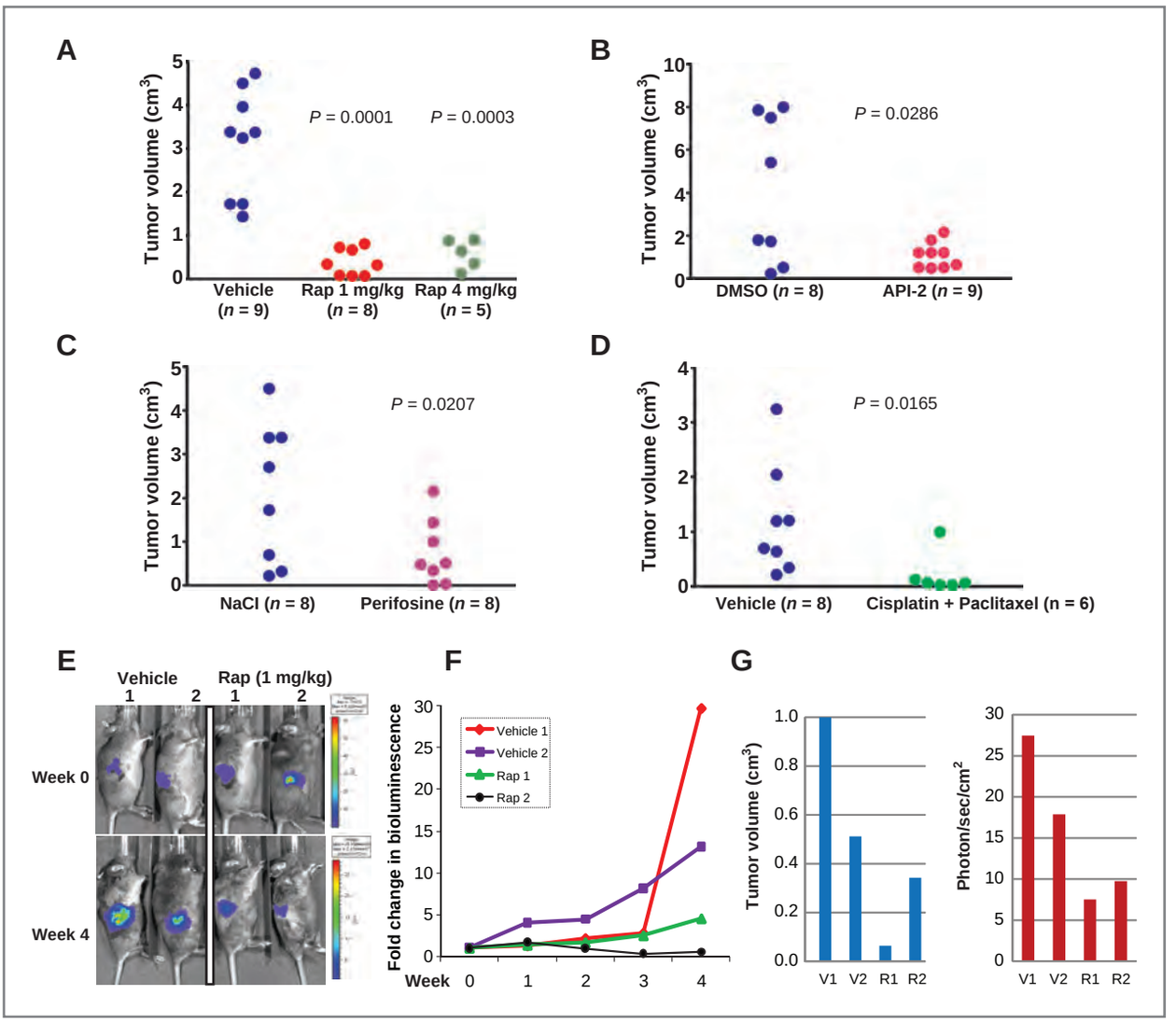

Figure 5. Inhibition of APC^{-}/PTEN^{-} murine ovarian tumor growth *in vivo* by conventional chemotherapy and drugs targeting activated PI3K/Akt/mTOR signaling. Small ovarian tumors present 6 weeks after AdCre injection were treated for 4 weeks with vehicle or rapamycin (1 mg/kg and 4 mg/kg; A), API-2 (B), perifosine (C), or cisplatin plus paclitaxel (D). Mice were euthanized at the end of the treatment period and right ovarian tumor volume was measured (length $\times$ width $\times$ height) using calipers. All treated groups showed significantly smaller tumors than controls. *P* values from 2-sample *t* tests on tumor volume are shown. E, bioluminescence imaging was done weekly in tumor-bearing animals treated with vehicle or rapamycin. Treatment was initiated 6 weeks after AdCre injection of the right ovarian bursae of *Apc*$^{flox/flox}$;*Pten*$^{flox/flox}$;*ROSA26* $^{L\text{-}S\text{-}L\text{-}luc/+}$ mice. Representative images before and after 4 weeks of treatment with rapamycin or vehicle are shown. Bioluminescence is indicated as photons/second/cm^2. Red signals correspond to maximal intensity, violet to minimal intensity, and other colors representing values in between. F, graph showing fold-change in luciferase activity based on BLI imaging of vehicle versus rapamycin-treated animals over the 4-week treatment course. G, comparison of tumor volume and BLI signal at study endpoint in vehicle and rapamycin-treated animals.

sections from tumors treated with rapamycin or vehicle (data not shown), and no significant difference was noted between the 2 groups. This finding is consistent with previous reports that rapamycin and its analogues can sensitize tumor cells in culture to cisplatin-induced apoptosis, but have minimal effects on apoptosis when used alone (28). Effects of cisplatin and paclitaxel on tumor cell proliferation and apoptosis could not be analyzed because residual tumor was identified in only 1 of 6 treated animals. Immunoblotting and IHC staining were used to analyze residual APC^{-}/PTEN^{-} tumors remaining after 4 weeks of treatment with rapamycin. Only small amounts of tumor tissue remained after treatment, limiting the number of studies that could be done. We found that pS6 (Ser235/236) levels were lower, and pAKT levels slightly increased, in rapamycin-treated tumors compared with those receiving vehicle (Supplementary Fig. S3, top panel). IHC staining of residual tumor tissue confirmed significant reduction of pS6 in the rapamycin-treated tumors compared with controls (Supplementary Fig. S3, bottom panels).

Published OnlineFirst September 8, 2011; DOI:10.1158/1078-0432.CCR-11-1388

Table 2. Drug response of murine APC^{-}/PTEN^{-} ovarian cancers

Drug	Tumor volume (cm^3; mean ± SD)	Liver metastasis	Ascites
Rapamycin (4 mg/kg)	0.581 ± 0.336	0/5	0/5
Rapamycin (1 mg/kg)	0.386 ± 0.311	0/8	2/8
Vehicle	3.12 ± 1.226	2/9	5/9
API-2	1.078 ± 0.201	0/9	0/9
DMSO	4.126 ± 1.205	0/8	3/8
Perifosine	0.746 ± 0.263	0/8	0/8
NaCl	2.116 ± 0.569	1/8	1/8
Cisplatin + paclitaxel	0.218 ± 0.157	0/6	0/6
NaCl + DMSO	1.199 ± 0.357	0/8	3/8

Tumor imaging

The ability to noninvasively and quantitatively image localized and metastatic OEAs in live animals would permit repeated and accurate measurements of tumor burden, increasing statistical power and reducing the number of animals needed to test each therapeutic regimen. To show the feasibility of this approach, we further engineered our OEA model to include a luciferase reporter allele that can be activated by AdCre. Mice with a Cre-activatable form of firefly luciferase allele present at the ubiquitously expressed *Rosa26* locus were crossed with $Apc^{flox/flox}$;$Pten^{flox/flox}$ mice to generate $Apc^{flox/flox}$;$Pten^{flox/flox}$;$ROSA26^{L\text{-}S\text{-}L\text{-}Luc/+}$ mice (17). We conducted ovarian bursal injection of AdCre in $Apc^{flox/flox}$;$Pten^{flox/flox}$;$Rosa26^{L\text{-}S\text{-}L\text{-}Luc/+}$ mice and bioluminescence imaging (BLI) was used to monitor tumor response to rapamycin therapy more than a 1-month course of treatment. Two tumor-bearing mice were treated with rapamycin (1 mg/kg) and 2 were treated with vehicle. BLI was carried out just before initiation of treatment 6 weeks after ovarian bursal injection of AdCre, and weekly for 1 month thereafter (Fig. 5E and F). Both vehicle-treated animals showed a substantial increase in tumor bioluminescence over the treatment interval, while bioluminescence in the rapamycin-treated mice increased only minimally in 1 mouse (Rap1) and decreased in the other mouse (Rap2). Comparison of tumor volume and BLI signal at study endpoint is shown in Fig. 5G.

MEK/ERK signaling is upregulated in response to AKT inhibition in murine APC^{-}/PTEN^{-} and human ovarian carcinoma cell lines

Recent findings imply a link between mTOR inhibition and ERK activation, possibly reflecting interruption of an S6K1-dependent negative feedback loop (29, 30). Moreover, simultaneous inhibition of mTOR and MEK/ERK signaling has been shown to substantially enhance antitumor effects *in vitro* and *in vivo* (31, 32). We tested whether inhibition of AKT signaling in murine and human ovarian cancer cell lines is associated with compensatory upregulation of MEK/ERK signaling. As expected, perifosine treatment for 2 hours resulted in a dose-dependent reduction of pAKT and pS6 in W2671T, W2830T, and A2780 cells (Fig. 6A and B). Notably, pERK was also substantially increased in all 3 cell lines following treatment with perifosine. Similar findings were noted in cells treated with API-2, including A2780 cells with and without mutant (S33Y) β-catenin (Fig. 6C and D). Upregulation of MEK/ERK signaling was also observed in rapamycin treated W2830T and TOV-112D cell lines (Fig. 6E and Supplementary Fig. S2A).

Discussion

Thus far, clinical trials of new drugs have relied heavily on preclinical studies testing drug effects on OvCa-derived cell lines in culture or xenografted into immune-compromised mice. These systems have a number of shortcomings, reviewed by Frese and Tuveson among others (33), and there is hope that genetically engineered mouse (GEM) models of OvCa will prove superior to cultured cells and tumor xenografts for testing the efficacy of novel therapeutic regimens. Existing GEM models of OvCa have been surprisingly underutilized for this purpose. In the studies presented here, we have focused on addressing the utility of a robust mouse OEA model, based on conditional inactivation of the *Apc* and *Pten* tumor suppressor genes in the ovarian surface epithelium, for preclinical testing of agents targeting activated PI3K/AKT/mTOR signaling.

Although many OEAs are low stage at diagnosis and have an excellent prognosis, a substantial fraction of OEAs present at FIGO stage III or IV. On the basis of a series of cases from which data were prospectively collected more than a 20-year period at a single center, 48% were high stage at diagnosis and these were associated with poor (less than 12%) 5-year progression-free survival after platinum-based therapy (34). It is reasonable to hope that drugs that target activated PI3K/Akt/mTOR signaling might prove to be useful for treating patients whose tumors harbor mutations that dysregulate this signaling pathway, particularly those with high stage disease or risk of recurrence. Given the modest number of patients with OEAs and the many drug combinations, doses, and schedules that could be explored in clinical trials, we hypothesized that our mouse OEA model might prove valuable for validating the concept of targeting PI3K/AKT/mTOR signaling in OEAs and in defining a limited number of higher priority agents and combinations. We report data here showing that agents targeting PI3K/AKT/mTOR signaling are active *in vitro* and *in vivo* against OEAs, and that longitudinal imaging approaches with luciferase-based reporters to measure tumor burden and dissemination might be particularly promising.

Platinum-taxane combination chemotherapy is well established as first-line therapy for advanced ovarian cancer, including OEAs (35). Initial response rates exceed 80%, but most patients relapse and response of recurrent disease to other agents such as doxorubicin, gemcitabine, topotecan,

Published OnlineFirst September 8, 2011; DOI:10.1158/1078-0432.CCR-11-1388

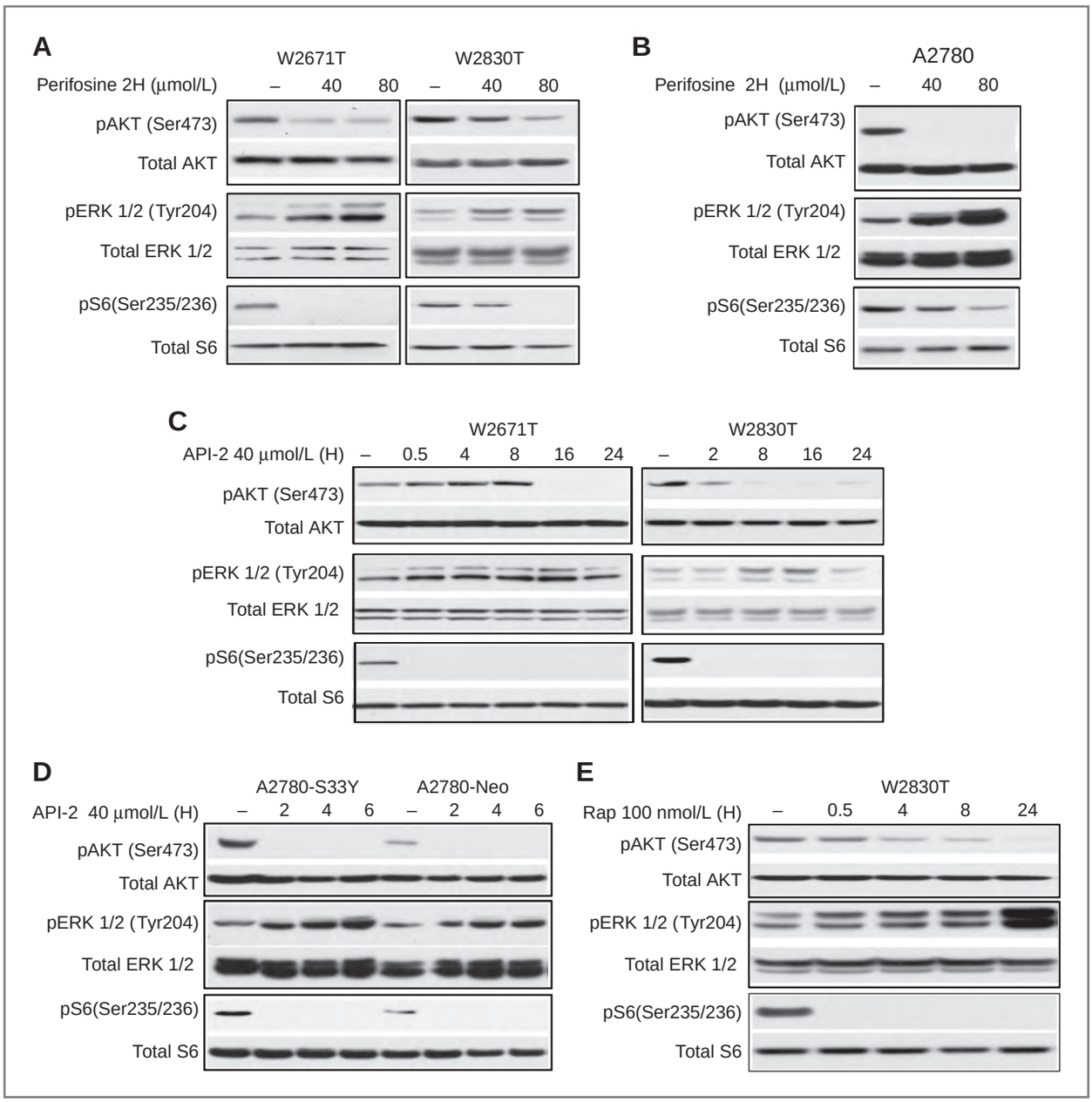

Figure 6. Akt inhibition in murine and human ovarian tumor cells results in compensatory activation of MEK/ERK signaling. Immunoblots of lysates from W2671T and W2830T (A) and A2780 cells (B) treated for 2 hours with varying doses of perifosine; W2671T and W2830T (C) and A2780-S33Y and A2780-Neo cells (D) treated with 40 μmol/L API-2 over the indicated time course; W2830T cells treated with 100 nmol/L rapamycin for up to 24 hours (E). In each blot, levels of phosphorylated and total Akt, ERK, and S6 are shown.

and etoposide is unpredictable. Moreover, the likelihood of response decreases with each subsequent relapse. Attempts to overcome chemoresistance following platinum/taxane therapy using different classes of chemotherapeutic agents in various combinations, doses, and schedules have led to only incremental improvements in overall survival. More recently, improved understanding of ovarian cancer biology and molecular genetics has led to the development of targeted therapies, several of which have been tested in clinical trials. These include agents that target angiogenesis, Erbb family members such as epidermal growth factor receptor and ERBB2, and α-FR (reviewed by Yap and colleagues; ref. 35). Although the PI3K/Akt/mTOR signaling pathway is frequently activated in human ovarian cancers, including OEAs as discussed above, clinical trials assessing the potential of PI3K, Akt, or mTOR inhibitors for treating ovarian cancer have been somewhat limited thus far. In a small (15 subject) phase I study of weekly temsirolimus

Published OnlineFirst September 8, 2011; DOI:10.1158/1078-0432.CCR-11-1388

(mTOR inhibitor also known as CCI-779) and topotecan for treatment of advanced or recurrent gynecologic malignancies—nearly half of which were ovarian cancers—there were no complete or partial responses. Furthermore, myelosuppression was found to be dose limiting for the combination, and patients who had received prior pelvic radiation were unable to tolerate the treatment (36). A phase II trial assessing temsirolimus as a single agent in patients with persistent or recurrent ovarian cancer showed modest effects, but progression-free survival was below the level that would warrant phase III studies in unselected patients (37). Interestingly, a phase II study of another mTOR inhibitor, everolimus, has shown encouraging results as a single agent for patients with recurrent endometrioid adenocarcinomas of the endometrium (38), which like OEAs, have frequent mutations that dysregulate PI3K/Akt/mTOR signaling. Our data, using both *in vitro* and *in vivo* model systems, suggest that Akt and mTOR inhibitors are likely to have efficacy for treating ovarian cancers with PI3K/Akt/mTOR pathway defects. Santiskulvong and colleagues recently showed that dual targeting of PI3K and mTOR inhibited growth of ovarian carcinomas arising in another murine GEM model based on conditional activation of a mutant *K-ras* allele and biallelic inactivation of *Pten* (39). Collectively, our data provide support for using GEM models of ovarian cancer to help preselect drug regimens with greatest promise for efficacy in human clinical trials. For example, such models could be used to help determine whether a given targeted agent is likely to be more effective given simultaneously with, or after conventional therapy. Toxicities likely to be dose limiting could also be identified.

A number of different modalities have been used to noninvasively image tumors in living animals, including those developing in the context of GEM models. These modalities include high resolution ultrasound (40), micro-computed tomography (micro-CT; ref. 41), micro-positron emission tomography (micro-PET; ref. 42), MRI (43), and BLI (44, 45). Although each modality has pros and cons, some of the advantages of BLI include its high sensitivity, relatively low cost, short image acquisition times and relative ease of use with minimal image postprocessing requirements (44). Our model system has been engineered such that the luciferase reporter is synchronously activated when *Pten* and *Apc* are inactivated, allowing tumors to be monitored longitudinally over time with BLI, essentially from their inception. We have also shown that BLI can be effectively used to monitor effects of therapy.

The PI3K/AKT/mTOR and MEK/ERK signaling pathways likely cooperate in many tumor types to drive tumor growth, promote tumor cell survival and mediate resistance to therapy. Simultaneous inhibition of both pathways with targeted agents has been shown to substantially enhance antitumor effects *in vitro* and *in vivo* (31, 32, 46). Similar to our findings in OEA-derived cell lines, Rahmani and colleagues showed that treatment of leukemia cells with perifosine, which inhibits PI3K/Akt/mTOR signaling upstream of mTORC1, also induced Erk activation (47). Notably, combined treatment with the Mek inhibitor PD184352 and perifosine strikingly induced apoptosis in multiple malignant human hematopoietic cells. Although effects of Akt and mTOR inhibition on Erk activation may vary with cell type and context, our data suggest that clinical trials involving the use of targeted agents for ovarian cancers with activated PI3K/Akt/mTOR signaling should focus not only on improving the activity of conventional cytotoxic drugs by combining them with targeted agents, but also on designing rational combinations of targeted agents that inhibit complementary or compensatory cell survival pathways. We anticipate that animal models such as the one described here should facilitate identification of the most successful combination therapies for subsequent evaluation in clinical trials.

Disclosure of Potential Conflicts of Interest

No potential conflicts of interest were disclosed.

Grant Support

This work was supported by grants from the National Cancer Institute (RO1 CA4172) and the Department of Defense Ovarian Cancer Research Program (W81XWH-08-1-0453).

The costs of publication of this article were defrayed in part by the payment of page charges. This article must therefore be hereby marked *advertisement* in accordance with 18 U.S.C. Section 1734 solely to indicate this fact.

Received May 31, 2011; revised August 24, 2011; accepted August 30, 2011; published OnlineFirst September 8, 2011.

References

1. Seidman JD, Horkayne-Szakaly I, Haiba M, Boice CR, Kurman RJ, Ronnett BM. The histologic type and stage distribution of ovarian carcinomas of surface epithelial origin. Int J Gynecol Pathol 2004;23:41–4.
2. Jemal A, Siegel R, Xu J, Ward E. Cancer statistics, 2010. CA Cancer J Clin 2010;60:277–300.
3. Kurman RJ, Shih IeM. Pathogenesis of ovarian cancer: lessons from morphology and molecular biology and their clinical implications. Int J Gynecol Pathol 2008;27:151–60.
4. Shih IeM, Kurman RJ. Ovarian tumorigenesis: a proposed model based on morphological and molecular genetic analysis. Am J Pathol 2004;164:1511–8.
5. Seidman JD, Cho KR, Ronnett BM, Kurman RJ. Surface epithelial tumors of the ovary. In: Kurman RJ, Ellenson LH, Ronnett BM, editors. Blaustein's pathology of the female genital tract. 6th ed. New York: Springer; 2011.
6. Ahmed AA, Etemadmoghadam D, Temple J, Lynch AG, Riad M, Sharma R, et al. Driver mutations in TP53 are ubiquitous in high grade serous carcinoma of the ovary. J Pathol 2010;221:49–56.
7. Wu R, Hendrix-Lucas N, Kuick R, Zhai Y, Schwartz DR, Akyol A, et al. Mouse model of human ovarian endometrioid adenocarcinoma based on somatic defects in the Wnt/B-catanin and PI3K/Pten signaling pathways. Cancer Cell 2007;11:321–33.

Published OnlineFirst September 8, 2011; DOI:10.1158/1078-0432.CCR-11-1388

8. Cho KR, Shih IM. Ovarian cancer. Annu Rev Pathol Mech Dis 2009;4:287–313.
9. McCluggage WG. My approach to and thoughts on the typing of ovarian carcinomas. J Clin Pathol 2008;61:152–63.
10. Wiegand KC, Shah SP, Al-Agha OM, Zhao Y, Tse K, Zeng T, et al. ARID1A mutations in endometriosis-associated ovarian carcinomas. N Engl J Med 2010;363:1532–43.
11. Shibata H, Toyama K, Shioya H, Ito M, Hirota M, Hasegawa S, et al. Rapid colorectal adenoma formation initiated by conditional targeting of the Apc gene. Science 1997;278:120–3.
12. Suzuki A, Yamaguchi MT, Ohteki T, Sasaki T, Kaisho T, Kimura Y, et al. T cell-specific loss of Pten leads to defects in central and peripheral tolerance. Immunity 2001;14:523–34.
13. Roby KF, Taylor CC, Sweetwood JP, Cheng Y, Pace JL, Tawfik O, et al. Development of a syngeneic mouse model for events related to ovarian cancer. Carcinogenesis 2000;21:585–91.
14. Wu R, Zhai Y, Fearon ER, Cho KR. Diverse mechanisms of beta-catenin deregulation in ovarian endometrioid adenocarcinomas. Cancer Res 2001;61:8247–55.
15. Saito M, Okamoto A, Kohno T, Takakura S, Shinozaki H, Isonishi S, et al. Allelic imbalance and mutations of the PTEN gene in ovarian cancer. Int J Cancer 2000;85:160–5.
16. Kolligs FT, Hu G, Dang CV, Fearon ER. Neoplastic transformation of RK3E by mutant beta-catenin requires deregulation of Tcf/Lef transcription but not activation of c-myc expression. Mol Cell Biol 1999;19:5696–706.
17. Safran M, Kim WY, Kung AL, Horner JW, DePinho RA, Kaelin WG Jr. Mouse reporter strain for noninvasive bioluminescent imaging of cells that have undergone Cre-mediated recombination. Mol Imaging 2003;2:297–302.
18. Mandai M, Yamaguchi K, Matsumura N, Baba T, Konishi I. Ovarian cancer in endometriosis: molecular biology, pathology, and clinical management. Int J Clin Oncol 2009;14:383–91.
19. Hideshima T, Catley L, Yasui H, Ishitsuka K, Raje N, Mitsiades C, et al. Perifosine, an oral bioactive novel alkylphospholipid, inhibits Akt and induces *in vitro* and *in vivo* cytotoxicity in human multiple myeloma cells. Blood 2006;107:4053–62.
20. Choo AY, Blenis J. Not all substrates are treated equally: implications for mTOR, rapamycin-resistance and cancer therapy. Cell Cycle 2009;8:567–72.
21. Dowling RJ, Topisirovic I, Fonseca BD, Sonenberg N. Dissecting the role of mTOR: lessons from mTOR inhibitors. Biochim Biophys Acta 2010;1804:433–9.
22. Chen XG, Liu F, Song XF, Wang ZH, Dong ZQ, Hu ZQ, et al. Rapamycin regulates Akt and ERK phosphorylation through mTORC1 and mTORC2 signaling pathways. Mol Carcinog 2010;49:603–10.
23. Sarbassov DD, Ali SM, Sengupta S, Sheen JH, Hsu PP, Bagley AF, et al. Prolonged rapamycin treatment inhibits mTORC2 assembly and Akt/PKB. Mol Cell 2006;22:159–68.
24. She QB, Halilovic E, Ye Q, Zhen W, Shirasawa S, Sasazuki T, et al. 4E-BP1 is a key effector of the oncogenic activation of the AKT and ERK signaling pathways that integrates their function in tumors. Cancer Cell 2010;18:39–51.
25. Inoki K, Ouyang H, Zhu T, Lindvall C, Wang Y, Zhang X, et al. TSC2 integrates Wnt and energy signals via a coordinated phosphorylation by AMPK and GSK3 to regulate cell growth. Cell 2006;126:955–68.
26. Yang L, Dan HC, Sun M, Liu Q, Sun XM, Feldman RI, et al. Akt/protein kinase B signaling inhibitor-2, a selective small molecule inhibitor of Akt signaling with antitumor activity in cancer cells overexpressing Akt. Cancer Res 2004;64:4394–9.
27. Fu L, Kim YA, Wang X, Wu X, Yue P, Lonial S, et al. Perifosine inhibits mammalian target of rapamycin signaling through facilitating degradation of major components in the mTOR axis and induces autophagy. Cancer Res 2009;69:8967–76.
28. Beuvink I, Boulay A, Fumagalli S, Zilbermann F, Ruetz S, O'Reilly T, et al. The mTOR inhibitor RAD001 sensitizes tumor cells to DNA-damaged induced apoptosis through inhibition of p21 translation. Cell 2005;120:747–59.
29. Grant S. Cotargeting survival signaling pathways in cancer. J Clin Invest 2008;118:3003–6.
30. Aksamitiene E, Kholodenko BN, Kolch W, Hoek JB, Kiyatkin A. PI3K/Akt-sensitive MEK-independent compensatory circuit of ERK activation in ER-positive PI3K-mutant T47D breast cancer cells. Cell Signal 2010;22:1369–78.
31. Carracedo A, Ma L, Teruya-Feldstein J, Rojo F, Salmena L, Alimonti A, et al. Inhibition of mTORC1 leads to MAPK pathway activation through a PI3K-dependent feedback loop in human cancer. J Clin Invest 2008;118:3065–74.
32. Kinkade CW, Castillo-Martin M, Puzio-Kuter A, Yan J, Foster TH, Gao H, et al. Targeting AKT/mTOR and ERK MAPK signaling inhibits hormone-refractory prostate cancer in a preclinical mouse model. J Clin Invest 2008;118:3051–64.
33. Frese KK, Tuveson DA. Maximizing mouse cancer models. Nat Rev Cancer 2007;7:645–58.
34. Storey DJ, Rush R, Stewart M, Rye T, Al-Nafussi A, Williams AR, et al. Endometrioid epithelial ovarian cancer: 20 years of prospectively collected data from a single center. Cancer 2008;112:2211–20.
35. Yap TA, Carden CP, Kaye SB. Beyond chemotherapy: targeted therapies in ovarian cancer. Nat Rev Cancer 2009;9:167–81.
36. Temkin SM, Yamada SD, Fleming GF. A phase I study of weekly temsirolimus and topotecan in the treatment of advanced and/or recurrent gynecologic malignancies. Gynecol Oncol 2010;117:473–6.
37. Behbakht K, Sill MW, Darcy KM, Rubin SC, Mannel RS, Waggoner S, et al. Phase II trial of the mTOR inhibitor, temsirolimus and evaluation of circulating tumor cells and tumor biomarkers in persistent and recurrent epithelial ovarian and primary peritoneal malignancies: A Gynecologic Oncology Group study. Gynecol Oncol 2011;123:19–26.
38. Slomovitz BM, Lu KH, Johnston T, Coleman RL, Munsell M, Broaddus RR, et al. A phase 2 study of the oral mammalian target of rapamycin inhibitor, everolimus, in patients with recurrent endometrial carcinoma. Cancer 2010;116:5415–9.
39. Santiskulvong C, Konecny GE, Fekete M, Chen KY, Karam A, Mulholland D, et al. Dual targeting of phosphoinositide 3-kinase and mammalian target of rapamycin using NVP-BEZ235 as a novel therapeutic approach in human ovarian carcinoma. Clin Cancer Res 2011;17:2373–84.
40. Cook N, Olive KP, Frese K, Tuveson DA. K-Ras-driven pancreatic cancer mouse model for anticancer inhibitor analyses. Methods Enzymol 2008;439:73–85.
41. Singh M, Lima A, Molina R, Hamilton P, Clermont AC, Devasthali V, et al. Assessing therapeutic responses in Kras mutant cancers using genetically engineered mouse models. Nat Biotechnol 2010;28:585–93.
42. Pestourie C, Theze B, Kuhnast B, Le Helleix S, Gombert K, Dolle F, et al. PET imaging of medullary thyroid carcinoma in MEN2A transgenic mice using 6-[(18)F]F-L-DOPA. Eur J Nucl Med Mol Imaging 2010;37:58–66.
43. Hensley H, Quinn BA, Wolf RL, Litwin SL, Mabuchi S, Williams SJ, et al. Magnetic resonance imaging for detection and determination of tumor volume in a genetically engineered mouse model of ovarian cancer. Cancer Biol Ther 2007;6:1717–25.
44. O'Neill K, Lyons SK, Gallagher WM, Curran KM, Byrne AT. Bioluminescent imaging: a critical tool in pre-clinical oncology research. J Pathol 2010;220:317–27.
45. Connolly DC, Hensley HH. Xenograft and transgenic mouse models of epithelial ovarian cancer and non invasive imaging modalities to monitor ovarian tumor growth in situ–Applications in Evaluating Novel Therapeutic Agents. Curr Protoc Pharmacol 2009;45:14.12.1–14.12.26.
46. Villanueva J, Vultur A, Lee JT, Somasundaram R, Fukunaga-Kalabis M, Cipolla AK, et al. Acquired resistance to BRAF inhibitors mediated by a RAF kinase switch in melanoma can be overcome by cotargeting MEK and IGF-1R/PI3K. Cancer Cell 2010;18:683–95.
47. Rahmani M, Anderson A, Habibi JR, Crabtree TR, Mayo M, Harada H, et al. The BH3-only protein Bim plays a critical role in leukemia cell death triggered by concomitant inhibition of the PI3K/Akt and MEK/ERK1/2 pathways. Blood 2009;114:4507–16.

SUPPLEMENTAL FIGURE LEGENDS

Supplemental Figure S1. Characterization of W2671T and W2830T murine ovarian carcinoma cell lines.

Phase contrast photomicrographs showing epithelial-like cobblestone morphology of mouse ovarian carcinoma-derived cell lines A) W2671T and B) W2830T. W2671T cells are C) cytokeratin 8-positive by immunofluorescence staining and D) negative for vimentin. Inset shows vimentin-positive murine embryo fibroblast (MEF) cells used as a positive control.

Supplemental Figure S2. Characterization of PI3K/Akt/mTOR and Erk signaling pathway regulation in human ovarian cancer cells after treatment with mTOR inhibitor rapamycin.

Immunoblots showing dose-dependent effect of rapamycin (0.01 - 100nM) on phosphorylation of Akt, Erk, S6K1, S6, 4E-BP1, and GSK3β after exposure to rapamycin for 2 hours in A) TOV112D and B) A2780 cells transduced with mutant β-catenin (A2780-S33Y) or vector alone (A2780-Neo). Effects of rapamycin on the transcriptionally active (dephosphorylated on Ser37 or Thr41) form of β-catenin is also shown.

Supplemental Figure S3. Inhibition of S6 phosphorylation in APC^{-}/PTEN^{-} murine ovarian tumors by rapamycin in vivo

Immunoblot of lysates from primary tumor tissues from mice treated for 4 weeks with vehicle (V1, 2, 3), 1 mg/kg (R1) or 4 mg/kg (R4) rapamycin. Levels of phosphorylated and total Akt and S6, and β-actin are shown. Lower panels show IHC staining of primary tumor tissues for pS6 in vehicle (left) and rapamycin (right) treated murine ovarian tumors.

Figure S1

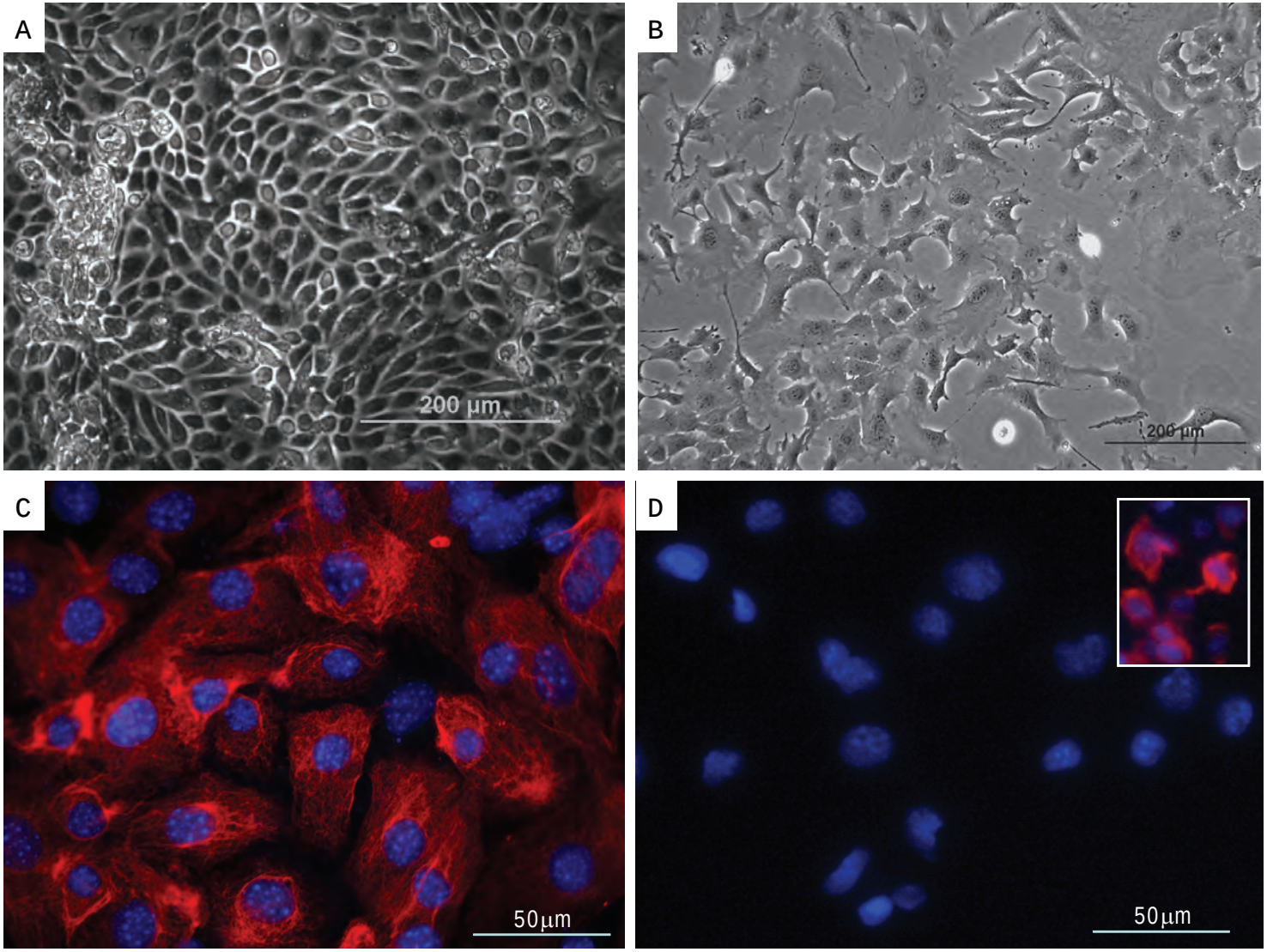

Figure S2

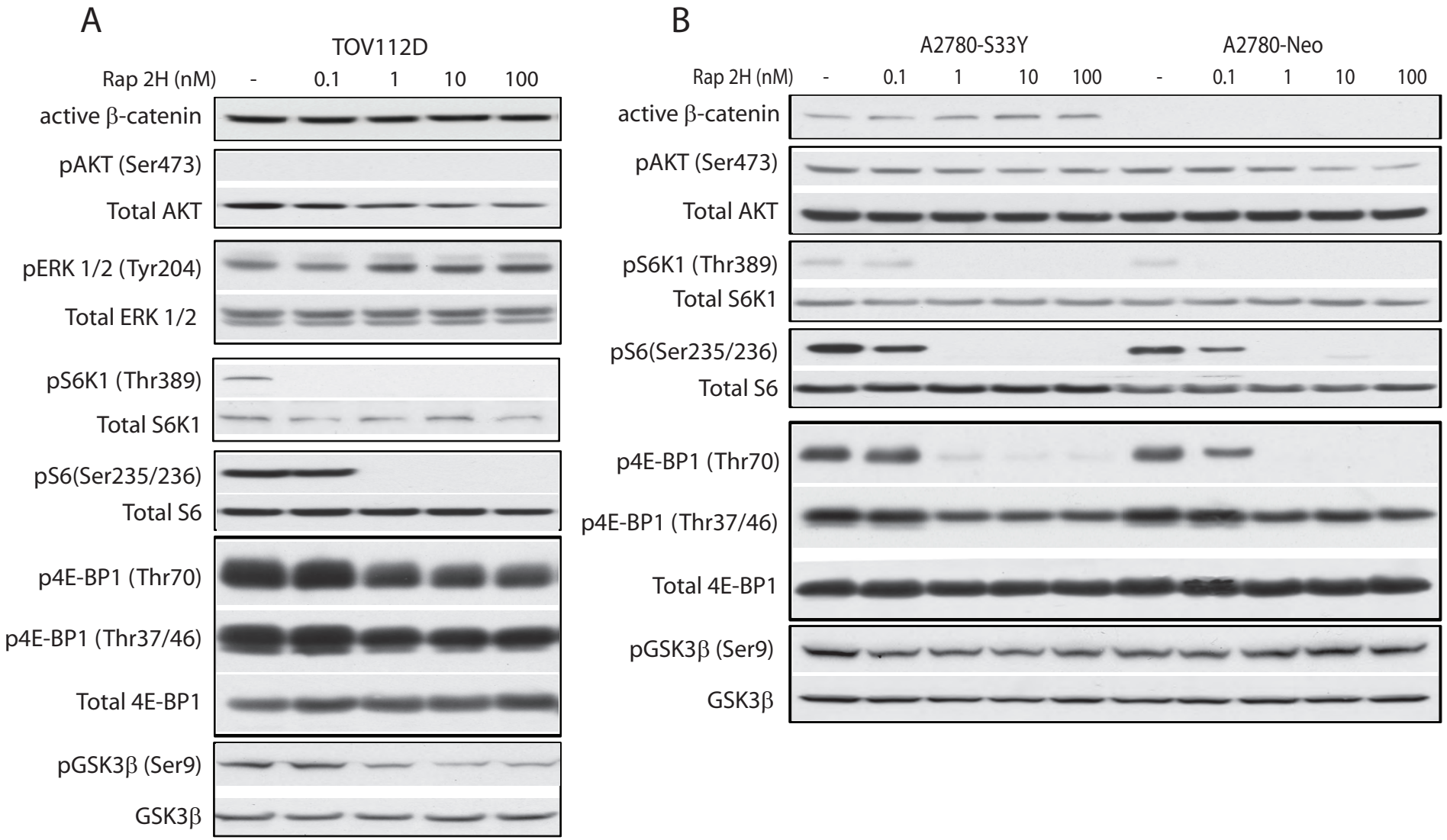
A
TOV112D
Rap 2H (nM) - 0.1 1 10 100
active β-catenin
pAKT (Ser473)
Total AKT
pERK 1/2 (Tyr204)
Total ERK 1/2
pS6K1 (Thr389)
Total S6K1
pS6(Ser235/236)
Total S6
p4E-BP1 (Thr70)
p4E-BP1 (Thr37/46)
Total 4E-BP1
pGSK3β (Ser9)
GSK3β
B
A2780-S33Y
A2780-Neo
Rap 2H (nM) - 0.1 1 10 100 - 0.1 1 10 100
active β-catenin
pAKT (Ser473)
Total AKT
pS6K1 (Thr389)
Total S6K1
pS6(Ser235/236)
Total S6
p4E-BP1 (Thr70)
p4E-BP1 (Thr37/46)
Total 4E-BP1
pGSK3β (Ser9)
GSK3β

Figure S3

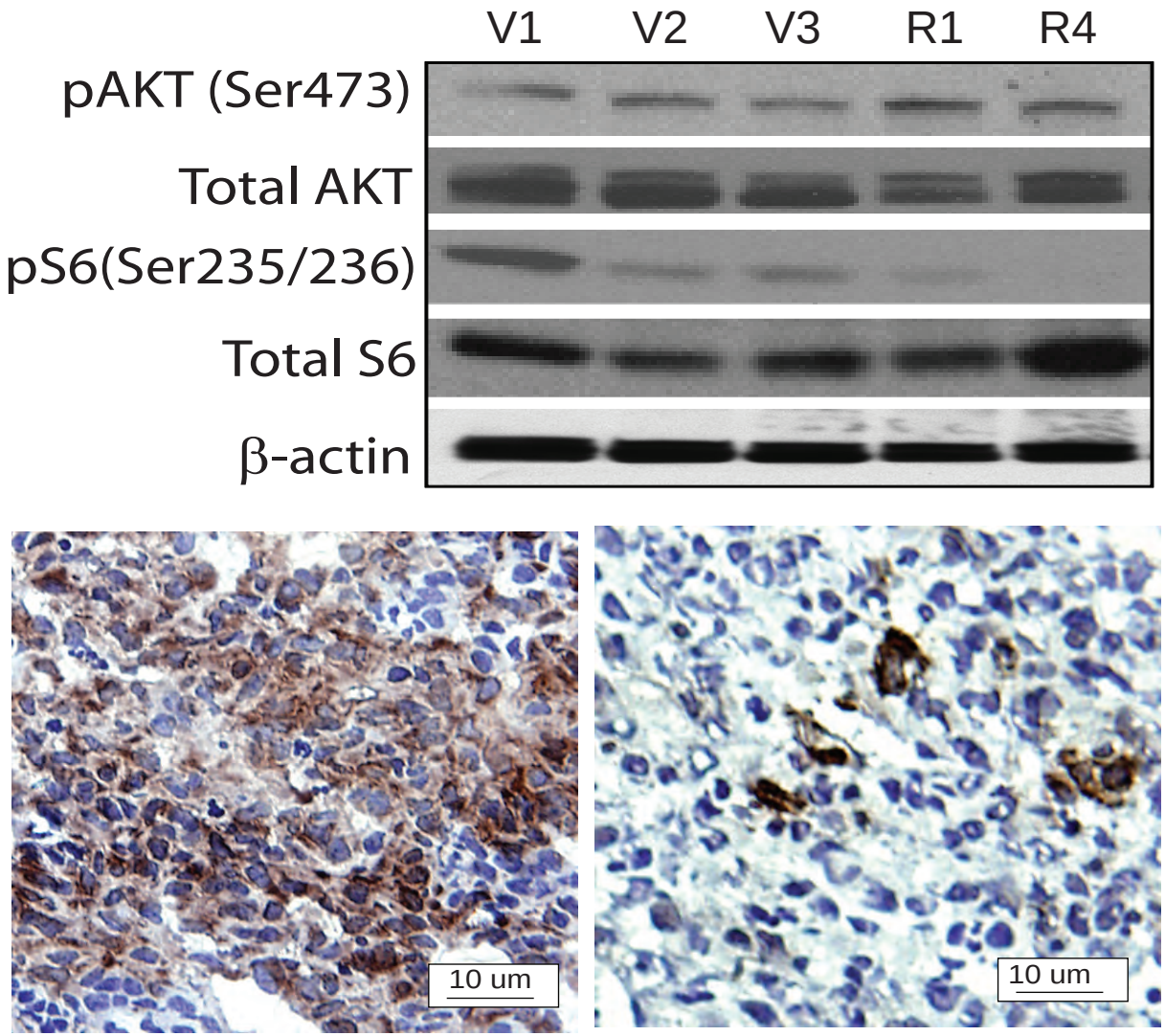
V1
V2
V3
R1
R4
pAKT (Ser473)
Total AKT
pS6(Ser235/236)
Total S6
β-actin
10 um
10 um

Abstract submitted for plenary lecture at the Japanese Society for Advancement of Women's Imaging (JSAWI) Annual Meeting, Awaji Island, Japan. September, 2011

Mouse Models for Imaging Ovarian Cancer Progression and Therapeutic Response: Progress and Pitfalls

Kathleen R. Cho, Departments of Pathology and Internal Medicine and the Comprehensive Cancer Center, University of Michigan Medical School, Ann Arbor, Michigan, U.S.A.

The traditional classification of ovarian carcinomas (OvCas), still widely used by diagnostic pathologists, relies entirely on the morphology of the neoplastic cells under the light microscope. In this scheme, most OvCas are classified into one of four major groups (serous, clear cell, endometrioid, or mucinous) based on how closely the tumor cells resemble non-neoplastic cells in other regions of the genital tract. However, accumulated clinicopathologic and molecular data have recently led to a new proposed model of OvCa pathogenesis in which tumors are broadly divided into two categories. The Type I OvCas are considered low grade, genetically stable, and relatively indolent tumors that frequently harbor somatic mutations that dysregulate specific cell signaling pathways. The Type I lesions include most endometrioid, clear cell, and mucinous OvCas as well as low grade serous carcinomas. In contrast, Type II OvCas are presumed to be high grade, biologically aggressive tumors from their outset, with a propensity for metastasis from small-volume and often clinically undetectable lesions. Most Type II OvCas are high grade serous carcinomas, virtually all of which harbor mutant *TP53* alleles. We have developed genetically engineered mouse (GEM) models of prototypical Type I and Type II-like OvCas which can be used to study the biology of tumor progression and metastasis. On-board imaging reporters have been incorporated into the model systems, allowing disease progression and therapeutic response to be monitored longitudinally in living animals. GEM model systems such as these are expected to enhance our understanding of Type I and Type II OvCa pathogenesis, and help accelerate the transition of the most promising new therapies for OvCa from the laboratory into clinical trials.

Cho, Kathleen

From: Mikhail Blagosklonny, MD, PhD <blagosklonny@oncotarget.com>
Sent: Saturday, November 12, 2011 6:38 PM
To: kathcho@umich.edu
Cc: Yelena Boryskina
Subject: To Dr. Cho from Cell Cycle

Dear Dr. Cho,

I am writing regarding your excellent paper "Preclinical Testing of PI3K/AKT/mTOR Signaling Inhibitors in a Mouse Model of Ovarian Endometrioid Adenocarcinoma"

Would you consider to write a brief FEATURE item (400-750 words, up to one figure (cartoon, no data) and up to 9 references)or Extra-View article (2000-5000 words, up to 140 references and as many figures as needed, including unpublished data),or, if you prefer, you may write a full-lenght review/perspective on a broad and/or different topic (2000-6000 words) for Cell Cycle

http://www.landesbioscience.com/journals/cc

Please note that Cell Cycle covers all topics in biology and medicine including unrelated to cell cycle research and has published numerous papers on rapamycin

As you might know, we invite authors of the most interesting recent papers for additional insights. You may include something that was not discussed in original paper. Some updates since the paper published. You may speculate on the topic as you wish. This article may be addressed to a wider readership. You may include original unpublished data. Cell Cycle is a traditional in print peer-reviewed journal covered by PubMed/Medline and ISI. Its launch coincided with the Nobel Prize to Paul Nurse who is a member of the Editorial Board, which also includes 20 members of the National Academy and 3 Nobel Prize winners.
Cell Cycle has published exciting articles by Irving Weissman, Charles Sherr, Arthur Pardee, Bert Vogelstein, Arnold Levine, Tony Hunter, RobertWeinberg, Susan Lindquist, Tim Hunt and other outstanding scientists

Please let us know so we could plan accordingly. What might be your time frame?
Please cc to: yelena@landesbioscience.com

With best wishes,
Mikhail

****

Dr. Yelena Boryskina, Assistant Editor
Prof. Mikhail V. Blagosklonny, Editor-in-Chief,
Cell Cycle
http://www.landesbioscience.com/journals/cc
&a mp;a mp;a mp;a mp;a mp;a mp;a mp;a mp;a mp;a mp;a mp;a mp;a mp;a mp;l t; /html>